



# Novel approach of multi-targeted thiazoles and thiazolidenes toward anti-inflammatory and anticancer therapy—dual inhibition of COX-2 and 5-LOX enzymes

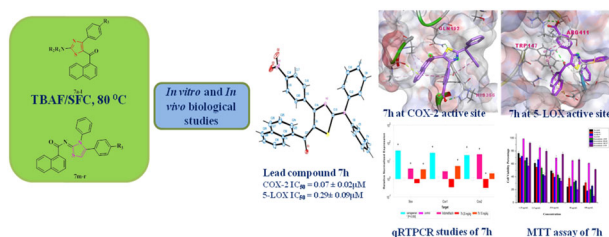
Jaismy Jacob P<sup>1</sup> · Manju S L<sup>1</sup>

Received: 3 August 2020 / Accepted: 15 October 2020  
© Springer Science+Business Media, LLC, part of Springer Nature 2020

## Abstract

It is well established that cyclooxygenase-2 (COX-2) and 5-lipoxygenase (5-LOX) play a vital role in the initiation and progression of inflammatory reactions. Hence, thiazole and thiazolidene-based pharmacophore molecules were synthesized to obtain dual COX-2 and 5-LOX inhibitory activity. The synthesis of target compounds has been achieved by a novel green strategy. In vitro COX-1, COX-2, and 5-LOX evaluation of these molecules have shown the potential for an improved anti-inflammatory profile. Most promising compound among the series (2-(diphenylamino)-4-(4-nitrophenyl)thiazol-5-yl) (naphthalen-1-yl)methanone **7h** ( $IC_{50} = 0.07 \pm 0.02 \mu\text{M}$ ) showed equivalent COX-2 inhibitory potency as that of positive control etoricoxib ( $IC_{50} = 0.07 \pm 0.01 \mu\text{M}$ ) and an enhanced selectivity index of 115.14. Compound **7h** exhibited 5-LOX  $IC_{50}$  of  $0.29 \pm 0.09 \mu\text{M}$  and reference drug zileuton showed  $IC_{50}$  of  $0.15 \pm 0.05 \mu\text{M}$ . In vivo studies of **7h** including carrageenan-induced paw edema assay (63% inhibition of paw edema), antiulcer studies, biochemical assays, qRT-PCR analysis, and anticancer studies indicated that the present study has identified a good lead compound for the development of a potential anti-inflammatory drug having improved gastric safety profile.

## Graphical Abstract



**Keywords** Thiazole · Cyclooxygenase-2 · 5-Lipoxygenase · Anti-inflammatory

## Introduction

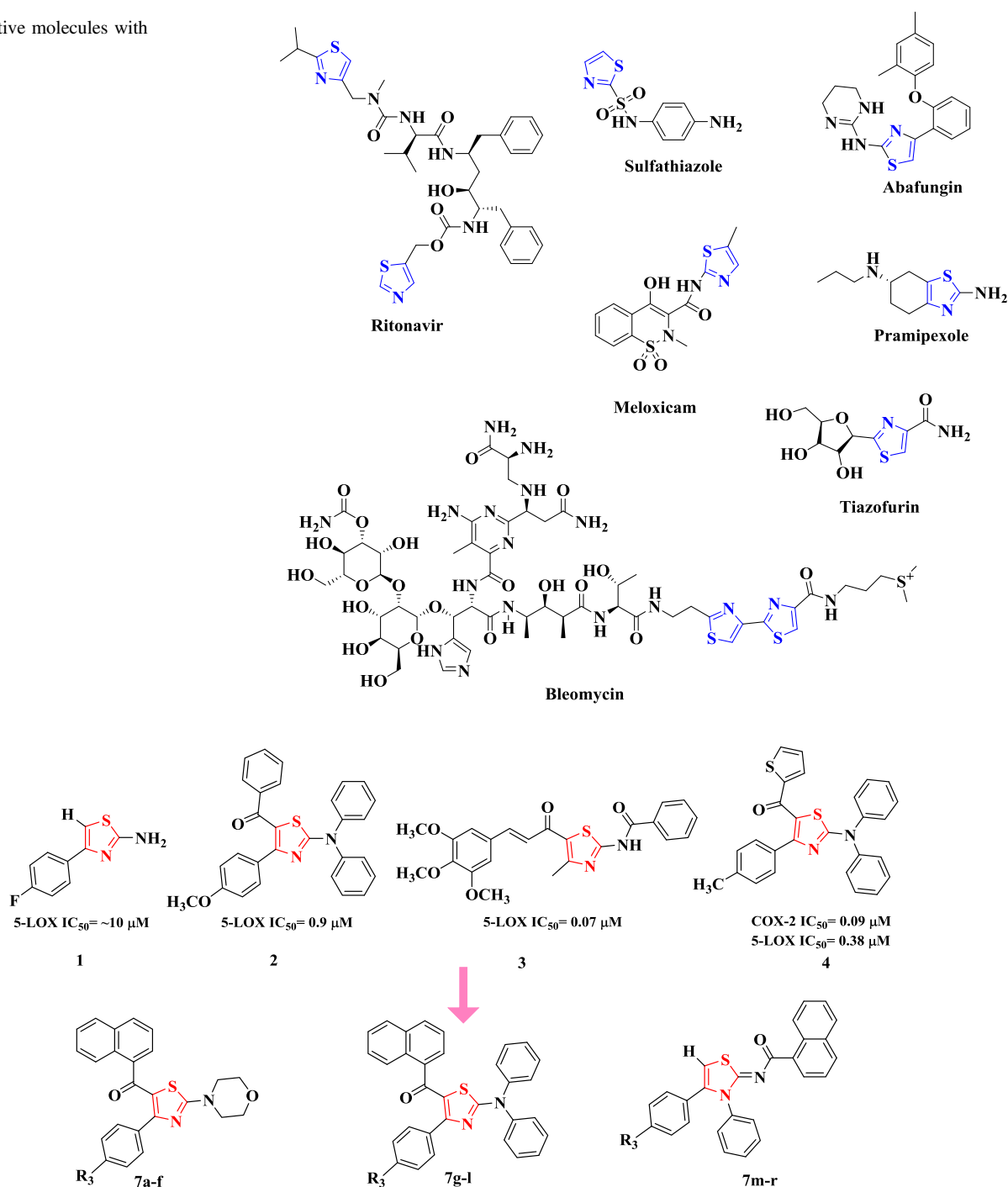
The significance of chronic inflammation in the pathophysiology of cancer, rheumatoid arthritis, cardiovascular, and neurological disorders is of serious therapeutic concern [1, 2]. Tumor microenvironments enclose a variety of inflammatory mediators, such as growth factors, chemokines, and cytokines that trigger extravasations of tumor cells [3]. Biologically, the protective response of the body to extrinsic and intrinsic stimuli is associated with alterations in arachidonic acid (AA) metabolism leading to

**Supplementary information** The online version of this article (<https://doi.org/10.1007/s00044-020-02655-9>) contains supplementary material, which is available to authorized users.

✉ Manju S L  
slmanju@vit.ac.in

<sup>1</sup> Department of Chemistry, School of Advanced Sciences, Vellore Institute of Technology, Vellore, Tamil Nadu, India

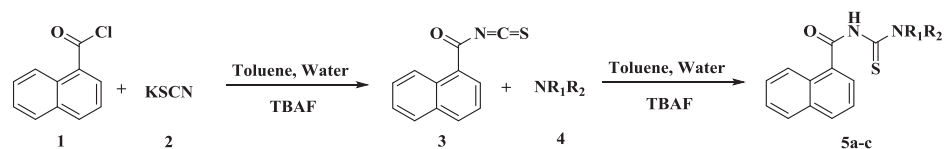
**Fig. 1** Bioactive molecules with thiazole ring



**Fig. 2** General structures of the novel molecules **7a–r** including previously reported 5-LOX inhibitors, **1**, **2**, **3**, and dual COX-2/5-LOX inhibitor, **4**, considered as the starting scaffolds for the design of new molecules.

inflammation. Cyclooxygenases (COX) and lipoxygenases (LOX) are two important enzymes involved in the AA cascade. COX include two isoenzymes, COX-1/COX-2, which produce prostaglandins (PGs), prostacyclin ( $PGI_2$ ), and thromboxanes from AA. Among the COXs, COX-1 is intrinsic and responsible for homeostatic function whereas COX-2 is an inducible enzyme and is over expressed in

inflammation and tissue damage. Evidence showed that leukotriene metabolites produced by LOX especially 5-LOX are associated with cardiovascular diseases and cancer [4, 5]. The significance of dual inhibition of COX-2 and 5-LOX is further underscored as they have been reported to be upregulated in various tumor types, including colon cancer, prostate cancer, breast cancer, and pancreatic cancer [6, 7].

**Scheme 1** Synthesis of 4-substituted-N-(amino-1-carbonothioyl)-1-naphthamide (**5a–c**) derivatives**Table 1** Reaction optimization<sup>a,b</sup>

Entry	Catalyst (equiv)	Solvent	Temp (°C)	Time (h)	Yield (%) <sup>b</sup>
1	–	Neat	RT	24	11
2	–	Neat	100	24	20
3	TBAF(0.1)	Neat	RT	12	56
4	TBAF(0.1)	Neat	60	5	75
5	TBAF(0.1)	Neat	80	1.5	94
6	TBAF(0.1)	Neat	100	1.5	86
7	TBAF(0.05)	Neat	80	1.5	62
8	TBAF(0.2)	Neat	80	1.5	94
9	TBAF(0.4)	Neat	80	1.5	94
10	NaF	Neat	80	1.5	46
11	KF	Neat	80	1.5	42
12	CsF	Neat	80	1.5	37
13	TBAB	Neat	80	1.5	69
14	TBAHSO <sub>4</sub>	Neat	80	1.5	55
15	CTAB	Neat	80	1.5	57
16	TBAF(0.1)	Water	80	1.5	87
17	TBAF(0.1)	Ethanol	80	1.5	82
18	TBAF(0.1)	Acetonitrile	80	1.5	76
19	TBAF(0.1)	DMF	80	1.5	0

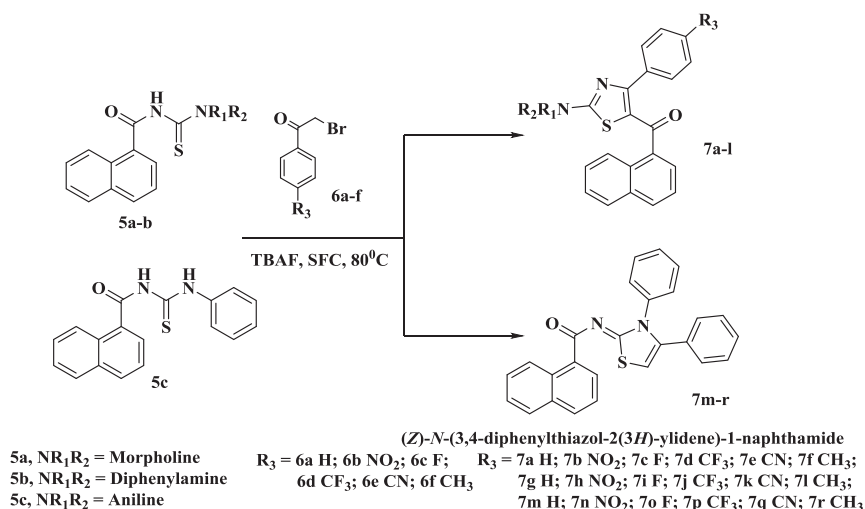
<sup>a</sup>Reagents and conditions: 1a (1.0 mmol), 2a (1.0 mmol), under solvent-free condition<sup>b</sup>Isolated yields

Epidemiologic investigations recommended that COX-2 inhibitors radically reduced the risk of these dreadful diseases [8]. Hence, multi-targeted ligands that inhibit both COX-2 and 5-LOX enzymes hold great promise in optimizing anti-inflammatory activity with minimal side effects [9]. Thus we have found the rationale for the extension of our research on COX-2/5-LOX inhibitors to cancer cell lines.

Thiazoles are important constituents of many naturally occurring biomolecules such as thiamine and synthetic drugs with a variety of therapeutic properties for instance analgesic, antipyretic, anti-inflammatory, anticancer, and antiviral activities [10–12]. Antiretroviral agent ritonavir

[13], antimicrobial agent sulfathiazole [14], antifungal agent abafungin [15], anti-inflammatory drug meloxicam [16], antiparkinson's drug pramipexole [17], and antineoplastic drug tiazofurin [18] and bleomycin [19] are few examples of clinically used thiazole-based drugs (Fig. 1). Interestingly, thiazol-4(5H)-one derivative darbufelone and 1,3-thiazolidine-2,4-dione derivative CI-987 are reported to possess dual COX/LOX inhibition [20]. Woods et al. reported the synthesis of thiazole analogues of indomethacin having selectivity toward COX-2, IC<sub>50</sub> ~ 0.3 nM [21]. Thiazolo-celecoxib analogues have been reported for COX-1/COX-2/15-LOX activity with IC<sub>50</sub> ~ 6.0, 2.0, and 5.0 μM, respectively [22]. Purine-pyrazole hybrids containing

**Scheme 2** Synthesis of 2-(substituted)-4-(4-substituted phenyl)thiazol-5-yl) (naphthalen-1-yl)methanone (**7a–l**) and N-(3-phenyl-4-(4-(substituted)phenyl)thiazol-2(3H)-ylidene)-1-naphthamide (**7m–r**) derivatives



thiazoles, thiazolidinones, and rhodanines, were reported to have 15-LOX IC<sub>50</sub> = 1.76–6.12 μM and potential anticancer and antioxidant activity [23].

Our group had reported 2-amino-4-aryl thiazoles [24], **1**, 2-amino-4-aryl thiazole-5-phenylmethanones [25], **2**, and N-(5-(3-substituted acryloyl)-4-methylthiazol-2-yl) benzamides [26], **3** as potent inhibitors of 5-LOX (Fig. 2). Recently, we have developed a new series of 2-carbonylthiophene substituted at the 5th position of thiazoles, **4** and thiazolidenes as potent dual inhibitors of COX-2/5-LOX with enhanced gastrointestinal tolerance and excellent in vivo anti-inflammatory activity [27] (Fig. 2). Encouraged by these results, it is envisaged that substitution of a bulky 1-naphthoyl moiety at 5th position of thiazoles would produce lead molecules with superior COX-2 inhibition and improved anti-inflammatory activities. We hereby report green synthesis of some 2-(alkyl/aromatic amino)-4-(4-substituted phenyl)thiazol-5-yl)(naphthalen-1-yl)methanone and N-(4-(4-substituted phenyl)-3-phenylthiazol-2(3H)-ylidene)-1-naphthamide and their in vitro evaluation for COX-1/COX-2 and 5-LOX inhibitory activity. Compounds with promising dual inhibitory activity were investigated for in vitro PGE<sub>2</sub> and LTB<sub>4</sub> inhibition. Besides, we conducted in vivo anti-inflammatory, antiulcer, qRT-PCR, and molecular docking studies on the most active compound. In the current study, the most active compound was also investigated for the anticancer activity on various cell lines.

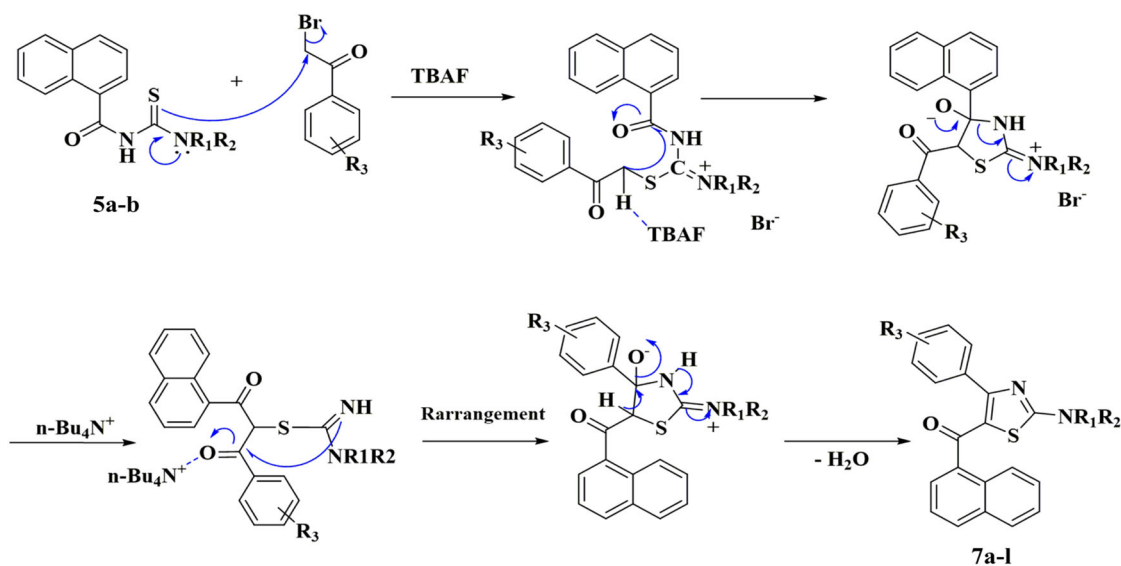
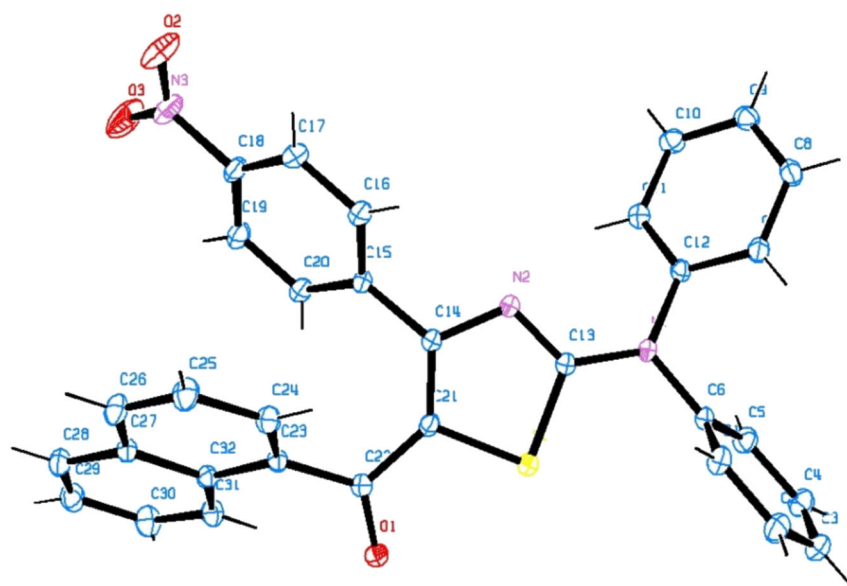
## Results and discussion

### Chemistry

Since thiazoles are associated with various biological activities and inspired by our earlier studies [25], here, we

intended to design and synthesis 2-amino-4-arylthiazol-5-yl)naphthalen-1-yl methanone derivatives. Naphthoyl moiety was introduced to the C<sub>5</sub> of thiazole ring, as the inclusion of a large aromatic ring would increase the bulkiness of the moiety, and henceforth it can fit well selectively within the large Val523 side pocket of the COX-2 active site. The key intermediate **5a–c** was synthesized with minor modification as per the earlier report [25]. Briefly, 1-naphthoyl thioureas (**5a–c**) in the first step were synthesized by treating 1-naphthoyl chloride with potassium thiocyanate in a toluene-water system in the presence of tetrabutylammonium fluoride (TBAF), followed by the reaction with substituted amines (Scheme 1). Initially, we optimized the reaction conditions for thiazole synthesis using the substrates, N-(diphenylcarbamothioyl)-1-naphthamide and 2-bromo-1-phenylethan-1-one to study the catalytic efficiency of TBAF. The results are shown in Table 1. Because of the low thermal stability of TBAF, reactions involving these were carried out below 100 °C [28]. Under SFC and in the absence of catalyst at RT, the reaction of N'-naphthoylthiourea with phenacyl bromide was negligible. Even after 24 h, the yield obtained was 11% (Table 1 entry 1). Then the temperature was raised to 100 °C, but there was no significant improvement in the reaction, 20% yield (Table 1 entry 2). However, after mixing of N'-naphthoylthiourea with phenacyl bromide in the presence of 0.1 equiv of TBAF at RT, thiazole was indeed formed in 1.5 h, 56% yield (Table 1 entry 3). Then, reaction at different temperatures such as 60, 80, and 100 °C was examined and the yield of product was gratifyingly increased to 75%, 94%, and 82%, respectively (Table 1 entries 4–6). These results emphasized the role of TBAF as a catalyst for cycloaddition. Further, we studied the effect of other fluoride catalysts such as NaF, KF, and CsF, which exhibited less catalytic activity compared to TBAF (Table 1 entries 10–12). Meanwhile, the study of other phase transfer catalysts like

**Fig. 3** Crystal structure of compound **7h**-ORTEP diagram, CCDC no. 1922521

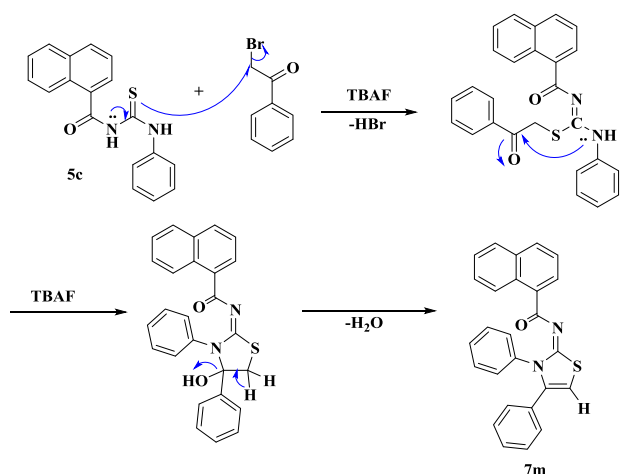


**Scheme 3** Proposed mechanism for the synthesis of compound **7a-l**

TBAB, TBAHSO<sub>4</sub>, and CTAB demonstrated that TBAF was the most useful catalyst amid them (Table 1 entries 13–15). 0.1 equiv of TBAF is optimal for the reaction as a further increase in catalyst concentration could not improve the yield (Table 1 entries 7–11). Both temperature and time of reaction were significant as the higher (100 °C) or lower (60 °C) temperature and reduction in reaction time reduced the yield. The effect of different solvents such as water, ethanol, acetonitrile, and dimethylformamide on yield was studied. The reaction in water and ethanol afforded comparably good yields of thiazole although it was less than SFC (Table 1 entries 16–19). By carrying out these experiments we established the best possible reaction procedure: adding 0.1 equiv of TBAF to equal moles of

N'-naphthoyl thiourea and phenacyl bromide under SFC and then carrying out the reaction at 80 °C for 1.5 h (Scheme 2).

In general, the electron-withdrawing substituents on *p*-position of phenacyl bromides afforded fast reaction rate and good yields. In this reaction the thiazole ring was formed by a rearrangement, as usual, we expected C-5 phenyl methanone substitution. To our surprise, we got naphthalenyl methanone substitution instead. The ORTEP figure of **7h**, (CCDC no. 1922521) is shown in Fig. 3. The formation of thiazole from thiourea and  $\alpha$ -halo ketone was rationalized mechanistically. Initially, the reaction was catalyzed by fluoride ion of TBAF, which activates the sulfur atom of thiourea and makes a stronger attack on the



**Scheme 4** Proposed mechanism for the synthesis of compound **7m–r**

active methylene group of phenacyl bromide. Then the N-C (4) bond fission supervenes and an open-chain intermediate was formed. Both the carbonyl groups are now susceptible to subsequent ring closure. Slow dehydration of the intermediate occurs through in situ activation of the PhCO group by  $n\text{Bu}_4\text{N}^+$  where more electrophilic carbonyl group predominates and 5-naphthalenyl methanone thiazole was formed in good yields (Scheme 3) [28–30]. Interestingly, this approach could provide a new way for the introduction of different C-5 substituents on the thiazole ring from aryl or heteroaryl acid chlorides [27]. On the other hand, thiazolidene derivatives were formed by another mechanism as shown in Scheme 4. Naphthylthiourea **5c** was activated in the presence of TBAF. The lone pair of electrons from amide nitrogen is transferred to the neighboring carbon following nucleophilic alkylation of thiourea with  $\alpha$ -bromoketones to form an intermediate, which could be cyclized to the desired compound after dehydration and proton transfer [27].

## Biological activity

### COX-1/2 inhibitory activity

All the compounds (**5a–c** and **7a–r**) were subjected to COX-2 inhibition studies and  $\text{IC}_{50}$  is shown in Table 2 with etoricoxib as a reference drug. During the COX reaction,  $\text{SnCl}_2$  reduces COX-derived  $\text{PGH}_2$  to  $\text{PGF}_{2\alpha}$  and was measured directly. The activity was determined by measuring the quantity of PG generated at various concentrations of test compounds by the enzyme. The activity was measured by calculating the selectivity index that was found out by the ratio of COX-1  $\text{IC}_{50}$  to COX-2  $\text{IC}_{50}$ , shown in Table 3. Further, compounds (**7d**, **7h**, **7n**, **7p**, **7r**) were chosen for COX-1  $\text{IC}_{50}$  determination by their considerable COX-2 and 5-LOX percentage inhibition. Among morpholine-substituted derivatives, compound **7d**

with  $p\text{-CF}_3$  phenyl showed superior activity. When a diphenylamino group was incorporated with  $p\text{-NO}_2$  phenyl ring to thiazole core, COX-2 selectivity was enhanced to  $\text{IC}_{50} = 0.07 \pm 0.02 \mu\text{M}$ , compound **7h**, while COX-1  $\text{IC}_{50}$  was  $8.06 \pm 0.11 \mu\text{M}$ . The most potent compound **7h** has a selectivity index of 115.14, which was superior to that of the selective COX-2 inhibitor, etoricoxib, 91.28. Besides, compound **7n** showed better selectivity to COX-2 than COX-1 with a selectivity index of 90.0. The exceptional selectivity of compounds **7h** and **7n** to COX-2 over COX-1 could be due to its naphthoyl group that provided bulkiness to the compound structure as COX-2 has a comparatively larger active site. Although the substitutions are being different, the  $p$ -phenyl substitution and tertiary amino group on the central thiazole core plays a key part in anti-inflammatory activity. In general, significant COX-2 inhibition was shown by compounds with an electron-withdrawing group ( $\text{NO}_2$ ,  $\text{CF}_3$ ) at  $p$ -position of the phenyl ring. Similarly, there was significant COX-2 inhibition associated with compounds substituted with  $p\text{-CH}_3$  phenyl ring (**7f**, **7l**, **7r**). Generally, naphthoyl substitution at C5 of thiazole ring improved COX-2 inhibition in comparison to previously reported thiophene derivatives [27].

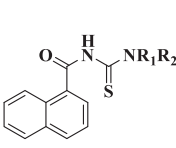
### 5-LOX inhibitory activity

The detection and measurement of hydroperoxides generated in the lipoxygenation reaction using purified 5-LOX enzyme are the basis of 5-LOX inhibitory assay. All the synthesized compounds were evaluated for soybean 5-LOX inhibitory activity and  $\text{IC}_{50}$  was determined. The results represented in Table 2 showed that compounds **7q** and **7r** with  $\text{IC}_{50} = 0.15 \pm 0.04 \mu\text{M}$  and  $0.16 \pm 0.01 \mu\text{M}$ , respectively have similar 5-LOX inhibition to that of standard zileuton ( $\text{IC}_{50} = 0.15 \pm 0.05 \mu\text{M}$ ). By analyzing 5-LOX activity and chemical structure of the compounds, it was observed that generally, the electron-withdrawing substitution at  $p$ -phenyl group may increase the 5-LOX inhibitory activity compared to the electron-donating groups. Besides, thiazoline derivatives (**7m–r**) have shown more affinity toward 5-LOX inhibition than thiazoles.

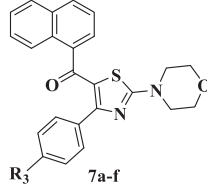
### PGE<sub>2</sub> and LTB<sub>4</sub> screening assay on LPS-induced RAW 264.7 cell lines

By lipopolysaccharide treatment (LPS) on RAW 264.7 cells, the concentration of PGE<sub>2</sub> and LTB<sub>4</sub> was markedly upregulated. PGE<sub>2</sub> and LTB<sub>4</sub> accumulation was increased to 1.28 and 0.92 ng/ml, respectively, following to LPS induction. All the compounds tested exhibited potential concentration-dependent inhibition of PGE<sub>2</sub> and LTB<sub>4</sub>, results depicted in Table 4. Most potent compound **7h** inhibited synthesis of PGE<sub>2</sub> at  $\text{IC}_{50} = 0.41 \pm 0.06 \mu\text{M}$  and LTB<sub>4</sub> at  $\text{IC}_{50} = 0.25 \pm 0.03$ . While, etoricoxib and zileuton

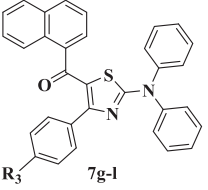
**Table 2** The IC<sub>50</sub> values of in vitro COX-2 and 5-LOX assay of compounds **5a–c**, **7a–r**, and reference drugs<sup>a</sup>



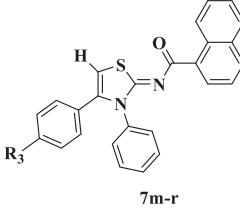
5a-c



7a-f



7g-l



7m-r

Sl no	Compound	R <sub>3</sub>	IC <sub>50</sub> ± SD (μM)	
			COX-2	5-LOX
1	<b>5a</b>	–	0.937 ± 0.005	11.34 ± 2.36
2	<b>5b</b> (Wu et al. [50])	–	5.08 ± 0.01	9.044 ± 0.42
3	<b>5c</b> (Bai et al. [51]; Dzurilla et al. [52]; Hemdan et al. [53])	–	10.61 ± 0.57	9.86 ± 0.69
4	<b>7a</b>	H	8.56 ± 0.19	7.77 ± 0.68
5	<b>7b</b>	NO <sub>2</sub>	8.26 ± 1.66	4.66 ± 0.75
6	<b>7c</b>	F	8.12 ± 0.52	5.61 ± 0.05
7	<b>7d</b>	CF <sub>3</sub>	0.28 ± 0.04	0.44 ± 0.73
8	<b>7e</b>	CN	8.54 ± 1.63	10.94 ± 0.37
9	<b>7f</b>	CH <sub>3</sub>	0.90 ± 0.064	14.28 ± 0.48
10	<b>7g</b>	H	6.04 ± 0.06	4.74 ± 0.95
11	<b>7h</b>	NO <sub>2</sub>	0.07 ± 0.02	0.29 ± 0.09
12	<b>7i</b>	F	0.931 ± 0.07	14.72 ± 1.0
13	<b>7j</b>	CF <sub>3</sub>	0.99 ± 0.11	4.74 ± 0.88
14	<b>7k</b>	CN	7.04 ± 0.37	4.97 ± 0.23
15	<b>7l</b>	CH <sub>3</sub>	0.77 ± 0.03	9.03 ± 0.66
16	<b>7m</b>	H	0.71 ± 0.05	5.10 ± 0.76
17	<b>7n</b>	NO <sub>2</sub>	0.08 ± 0.01	0.36 ± 0.05
18	<b>7o</b>	F	7.87 ± 0.14	0.26 ± 0.05
19	<b>7p</b>	CF <sub>3</sub>	0.71 ± 0.05	0.54 ± 0.02
20	<b>7q</b>	CN	10.27 ± 0.33	0.15 ± 0.04
21	<b>7r</b>	CH <sub>3</sub>	0.69 ± 0.46	0.16 ± 0.01
22	<b>Etoricoxib</b>	–	0.07 ± 0.01	–
23	<b>Zileuton</b>	–	–	0.15 ± 0.05

<sup>a</sup>IC<sub>50</sub> is the concentration of compound needed to produce 50% inhibition

**Table 3** IC<sub>50</sub> values and selectivity index (SI) of selected compounds against COX-1 and COX-2

Compound	IC <sub>50</sub> ± SD (μM)		Selectivity index (SI)
	COX-1	COX-2	
<b>7d</b>	6.92 ± 0.18	0.28 ± 0.04	24.71
<b>7h</b>	8.06 ± 0.11	0.07 ± 0.02	115.14
<b>7n</b>	7.20 ± 0.34	0.08 ± 0.01	90.0
<b>7p</b>	6.89 ± 0.26	0.71 ± 0.05	9.70
<b>7r</b>	6.87 ± 0.43	0.69 ± 0.46	9.95
<b>Etoricoxib</b>	6.39 ± 0.83	0.07 ± 0.01	91.28

 SI: IC<sub>50</sub> (COX-1)/IC<sub>50</sub> (COX-2)

**Table 4** PGE<sub>2</sub> and LTB<sub>4</sub> screening assay on LPS-induced RAW 264.7 cells

Compound	IC <sub>50</sub> ± SD (μM)	
	PGE <sub>2</sub>	LTB <sub>4</sub>
<b>7d</b>	0.49 ± 0.18	0.45 ± 0.09
<b>7h</b>	0.41 ± 0.06	0.25 ± 0.03
<b>7n</b>	0.61 ± 0.05	0.69 ± 0.13
<b>7p</b>	0.63 ± 0.09	0.53 ± 0.04
<b>7r</b>	0.68 ± 0.15	0.67 ± 0.03
<b>Etoricoxib</b>	0.46 ± 0.02	–
<b>Zileuton</b>	–	0.45 ± 0.10

exhibited PGE<sub>2</sub> inhibition and LTB<sub>4</sub> inhibition at IC<sub>50</sub> = 0.46 ± 0.02 μM and IC<sub>50</sub> = 0.45 ± 0.10 μM, respectively. This experiment suggested that these thiazole derivatives have excellent inhibitory potency toward PGE<sub>2</sub> and LTB<sub>4</sub>.

In vitro COX-2/5-LOX and PGE<sub>2</sub>/LTB<sub>4</sub> inhibition studies of the synthesized compounds showed a promising anti-inflammatory potential for compound **7h**. Therefore compound **7h** was selected for more studies.

### In vivo studies

The in vitro COX-1/2 and 5-LOX studies as well as PGE<sub>2</sub> and LTB<sub>4</sub> inhibitory studies on RAW 264.7 macrophage cells forecasted promising anti-inflammatory potential for compound **7h**. Hence the compound **7h** was chosen for further in vivo studies.

### Acute toxicity studies

As per OECD guidelines, in vivo acute toxicity studies on male Wistar rats were carried out to study the toxic effect of compound **7h**. Compound **7h** was orally administered to animals at 50, 500, and 2000-mg/kg doses. For the first 4 h, the animals were carefully monitored continuously for any signs of toxicity and then for the first 24 h at regular intervals. Subsequently, animals were observed once a day for 14 days. After 14 days, the animals were sacrificed and histological studies of liver, kidney, intestine, and stomach, showed no major structural difference compared to the control (Fig. 4).

### In vivo anti-inflammatory activity

The anti-inflammatory effect of compound **7h** was evaluated by Carrageenan-induced rat-paw edema method. Male Wistar rats were divided into different groups of five each. Group I consist of animals treated with vehicle, served as the control, and group II was administered with reference drug indomethacin (10 mg/kg). Group III and IV, were treated with test compound **7h** at 10, and 20 mg/kg, respectively, orally. 1% w/v carrageenan was administered by intraplantar injection 1 h after the treatment with the test compound or standard. The result was represented as percentage inhibition by measuring paw thickness at periods 1, 2, 4, and 6 h. Results of carrageenan-induced rat-paw edema were displayed in Fig. 5. The compound **7h** showed a 53% reduction in edema at 10-mg/kg dose (w.r.t control), which further improved significantly to 63% on raising the concentration to 20 mg/kg. Interestingly the effect of **7h** was comparable to that of standard drug, indomethacin (53% at 10 mg/kg dose).

### In vivo ulcerogenic activity

The use of NSAIDs for the treatment of inflammation was limited because of gastrointestinal side effects. Hence, compound **7h** with promising in vivo anti-inflammatory profile was further studied for its ulcerogenic activity. Subsequently, an oral dosage of **7h** (10 and 50 mg/kg) showed a normal gastrointestinal mucosal stomach architecture on gross observation. Whereas, administration of indomethacin at 10-mg/kg dose developed mucosal aberration and ulceration in rat stomach mucosa showing its severe ulcerative susceptibility. Besides, histopathological examination using hematoxylin and eosin stain revealed normal histology for rat stomach treated with **7h** while indomethacin treatment produced severe mucosal sloughing, lymphocytic, and granulation tissue infiltrate indicating potential ulceration affinity. Antiulcer studies ensured gastric safety along with the anti-inflammatory activity. See Fig. 6.

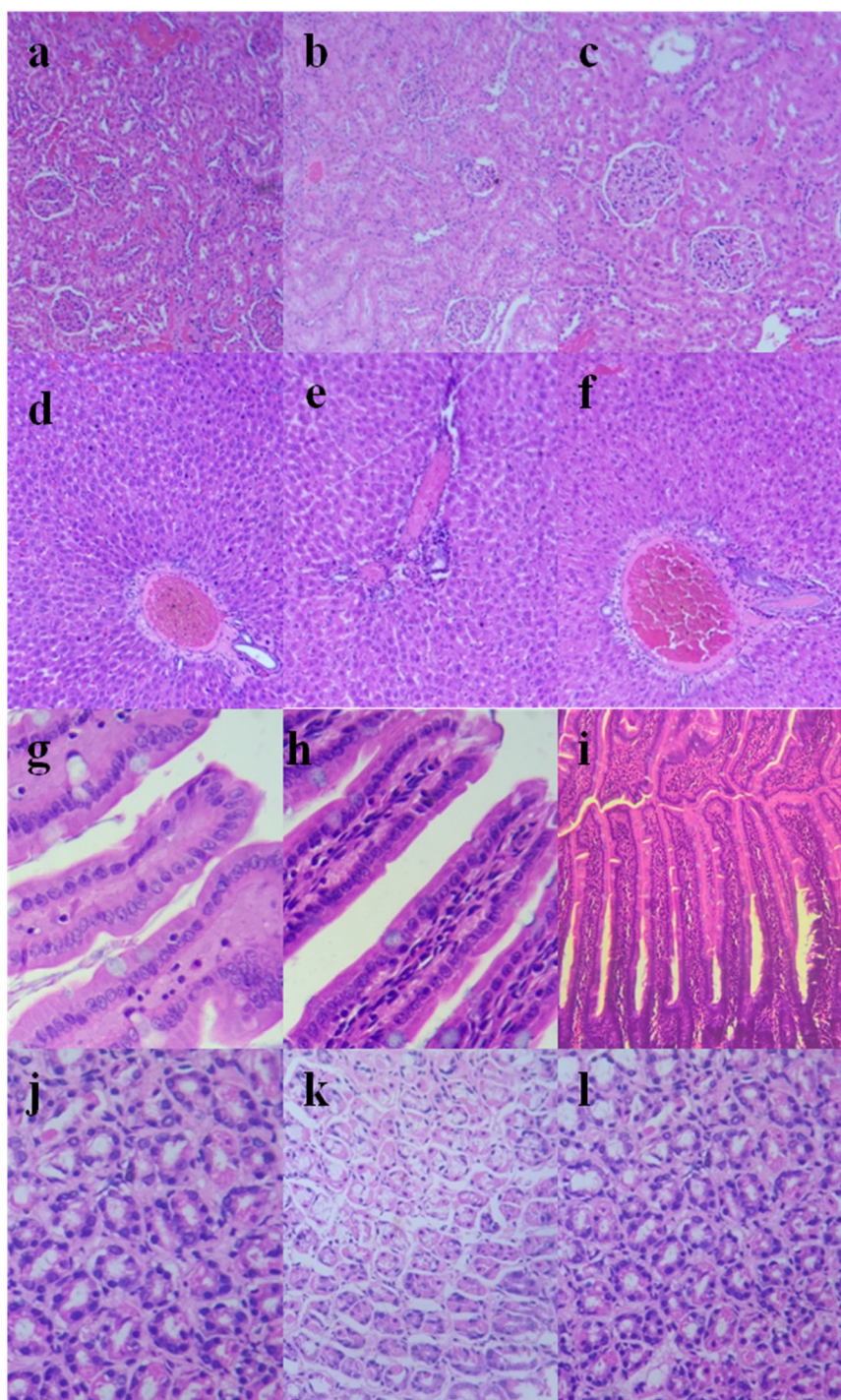
### PGE<sub>2</sub> and LTB<sub>4</sub> screening assay in rat-paw tissues

In addition to inhibiting rat-paw swelling, a range of biochemical assays confirmed the anti-inflammatory efficiency of compound **7h**. The hind-paw edema induced by carrageenan was associated with a noticeable rise in PGE<sub>2</sub> and LTB<sub>4</sub> concentrations. The PGE<sub>2</sub> level in the control group hind paws demonstrated a tenfold increase after carrageenan injection over 0–6 h. Similarly, during the same time interval, LTB<sub>4</sub> concentration was showed a sixfold increase. The concentration of both PGE<sub>2</sub> and LTB<sub>4</sub> was significantly reduced by pretreatment with compound **7h**. Compound **7h** exhibited a concentration-dependent decrease in PGE<sub>2</sub> and LTB<sub>4</sub> formation. Compound **7h** at 10 mg/kg inhibited the production of PGE<sub>2</sub> (786.29 ± 8.55 pg/mL) and LTB<sub>4</sub> (360.42 ± 7.7 pg/mL) more effectively than indomethacin 10 mg/kg (PGE<sub>2</sub>: 902.7 ± 11.03 pg/mL and LTB<sub>4</sub>: 374.14 ± 8.98 pg/mL) over the same period. The results are shown in Fig. 7.

### qRT-PCR studies

The qRT-PCR analysis was conducted on rat-paw tissue obtained after the anti-inflammatory studies to investigate the gene-level mechanism of inflammation inhibition by compound **7h**. Gene expression for COX-1/COX-2 and 5-LOX was upregulated at 28.50-, 21.27-, and 38.23-fold, respectively, than the housekeeping gene GAPDH, with carrageenan administration (Fig. 8). Gene expression in the presence of compound **7h** has significantly inhibited the upregulation of all the enzymes of interest. Besides, compared to indomethacin, compound **7h** considerably reduced the expression of each studied enzyme, particularly against COX-2. Results of qRT-PCR analysis could be well

**Fig. 4** **a, d, g, j** Histology of kidney, liver, intestine, and stomach, of control (400×). **b, e, h, k** Histology of kidney, liver, intestine, and stomach after treatment with compound **7h** 500 mg/kg. **c, f, i, l** Histology of kidney, liver, intestine, and stomach after treatment with compound **7h** administered at 2000-mg kg<sup>-1</sup> dose (400×)



correlated with anti-inflammatory activity and gastric protective action.

#### Anticancer study

In vitro cytotoxicity of compound **7h** was studied on L929 (Fibroblast) cells followed by in vitro anticancer activity on three cell lines (A549: human lung cancer, MCF-7: human

breast adenocarcinoma, DLD1: human colorectal adenocarcinoma) by the MTT assay. As shown in Fig. 9, target compound **7h** showed less anticancer activity against all the three cancer cell lines (IC<sub>50</sub>, A549: 24.29 ± 1.45 µg/mL, DLD1: 19.27 ± 1.16 µg/mL, MCF-7: 20.28 ± 3.04 µg/mL) compared to doxorubicin (IC<sub>50</sub>, A549: 14.59 ± 1.64 µg/mL, DLD1: 10.97 ± 1.14 µg/mL, MCF-7: 9.14 ± 1.45 µg/mL). Whereas compound **7h** displayed better safety profile

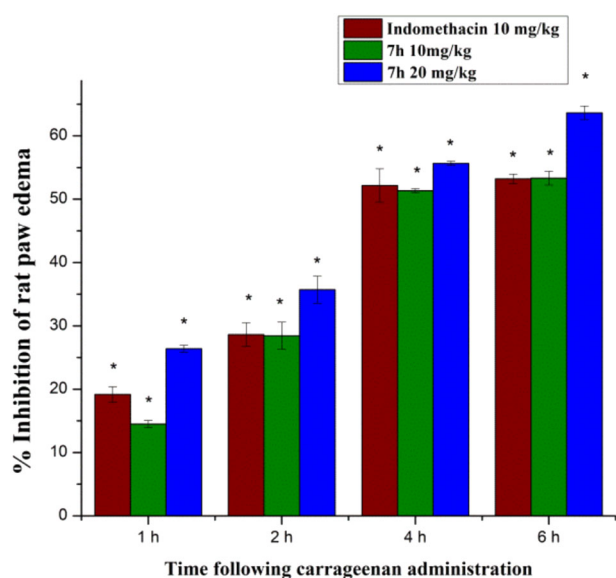


**Fig. 5** Effect of compound **7h** on percentage inhibition of rat-paw edema at different time intervals. All values are presented as the mean  $\pm$  SEM ( $n = 5$ ). Statistical significance has been calculated using one-way ANOVA. \* $p < 0.05$  vs. control group

toward L929 cells, normal cell line ( $IC_{50} = 110.24 \pm 3.53 \mu\text{g/mL}$ ) than doxorubicin ( $IC_{50} = 95.09 \pm 2.33 \mu\text{g/mL}$ ).

### Antioxidant activity

Reactive oxygen species (ROS) for instance superoxide radical, hydroxyl radical, and hydrogen peroxide are generated constantly in our body. The ROS can easily damage biomolecules including lipids, proteins, and DNA. Studies have suggested a close association between anti-inflammatory activity and radical scavenging. Compounds that inhibit the production of ROS have demonstrated a promising role in the management of inflammation and cancer [31]. Hence, we performed various antioxidant screening at  $20 \mu\text{M}$  for all the synthesized compounds. The results of the antioxidant study were displayed in Fig. 10.

### DPPH free radical scavenging assay

Anti-inflammatory agents, particularly 5-LOX inhibitors are found to be excellent radical scavengers. Therefore, the free radical scavenging activity of all the compounds synthesized was determined by the DPPH assay. The results displayed that all the compounds have less antioxidant activity showing  $\sim 58\%$  activity compared to the positive control, ascorbic acid ( $97.31 \pm 0.08\%$ ). Indomethacin and etoricoxib exhibited DPPH scavenging activity of  $55.49 \pm 0.93\%$  and  $57.19 \pm 0.27\%$ , respectively. Best COX-2/5-LOX inhibitor **7h** showed  $57.19 \pm 0.27\%$  inhibition. There was not much difference in the antioxidant activities

irrespective of various substitutions and we couldn't establish a correlation between anti-inflammatory potency and antioxidant activity.

### $\text{H}_2\text{O}_2$ radical scavenging assay

$\text{H}_2\text{O}_2$  is a type of ROS that is cytotoxic and genotoxic that is involved in various inflammatory conditions and disease pathogenesis.  $\text{H}_2\text{O}_2$  radical scavenging activity was studied for all the compounds. The highest  $\text{H}_2\text{O}_2$  inhibition was shown by compound **5b** ( $43.86 \pm 0.59\%$ ), followed by **7h**, which showed  $41.78 \pm 0.55\%$  scavenging activity. Reference drugs etoricoxib, indomethacin, and ascorbic acid had shown 9.24%, 49.45%, and 21.86% of  $\text{H}_2\text{O}_2$  scavenging activity, respectively.

### Iron-chelating assay

Chronic inflammatory processes trigger significant changes in iron metabolism and there are reports that iron in inflammatory synovial fluid is capable of producing hydroxyl radical. Accordingly, synovial iron leads to the progression of rheumatoid disease. Among all the compounds tested, **5c**, **7o**, **7g**, and ascorbic acid showed superior activity with  $\sim 31\%$  of iron-chelating. Compound **7h** and other reference drugs such as etoricoxib and indomethacin exhibited poor iron-chelating activity ( $\sim 7\%$ ).

### Nitric oxide (NO) radical scavenging assay

NO is harmful to various biomolecules, and elevated levels result in direct tissue toxicity and contribute to various inflammatory conditions and carcinomas. In this assay, many synthesized molecules were capable of scavenging NO significantly with  $\sim 65\%$  inhibition. Compound **7n** recorded the maximum scavenging with  $73.71 \pm 1.45\%$  and **7h** exhibited  $62.66 \pm 0.51\%$  NO scavenging. Whereas reference drugs such as etoricoxib and indomethacin had poor NO scavenging activity.

### Molecular docking study

In a docking study, the most active dual COX-2/5-LOX inhibitor **7h** was docked using AutoDockTools-1.5.6 into COX-2 and 5-LOX proteins. The 3D crystal structures of both COX-2 (pdb ID: 5IKT) and 5-LOX (pdb ID: 3O8Y) were obtained from the RCSB protein data bank. As depicted in Fig. 11, a hydrogen bond was formed between HIS356 and oxygen of nitro group (distance  $2.11 \text{ \AA}$ ). The sulfur atom of the thiazole ring was also found to establish hydrogen bonding interaction with GLN192. Apart from hydrogen bonds compound, **7h** formed pi-lone pair interaction and van der Waals interaction with PRO514 and

**Fig. 6** **A** Stomach histology of control rats, normal gastric mucosa (100×), **B** typical stomach architecture shows gastric pits (arrow) (200×), **C** typical adjoining gastric mucosa, (400×). **2.** Stomach histology of treated rats, **7h**, 50 mg/kg (**D**) shows typical gastric mucosa (100×), **E** normal stomach architecture shows gastric pits (arrow) (200×), **F** showing typical gastric mucosa, no evidence of gastric ulceration, (400×). **3.** Stomach histology of rats on indomethacin dosing, 10 mg/kg (**G**) Gastric mucosa showing ulceration (a), surface mucosal sloughing (b), presence of chronic inflammatory infiltrate (c) (arrows), (100×), **H** infiltrate of mucosal lymphocytes indicating the development of chronic gastritis, (arrows) (400×), **I** inflammatory granulation tissue with ulceration, (400×)

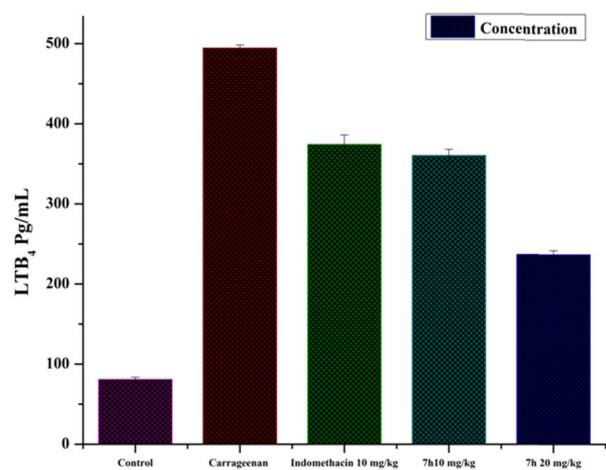
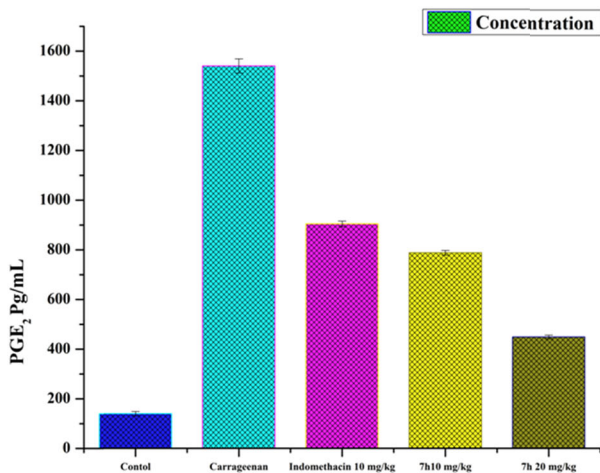
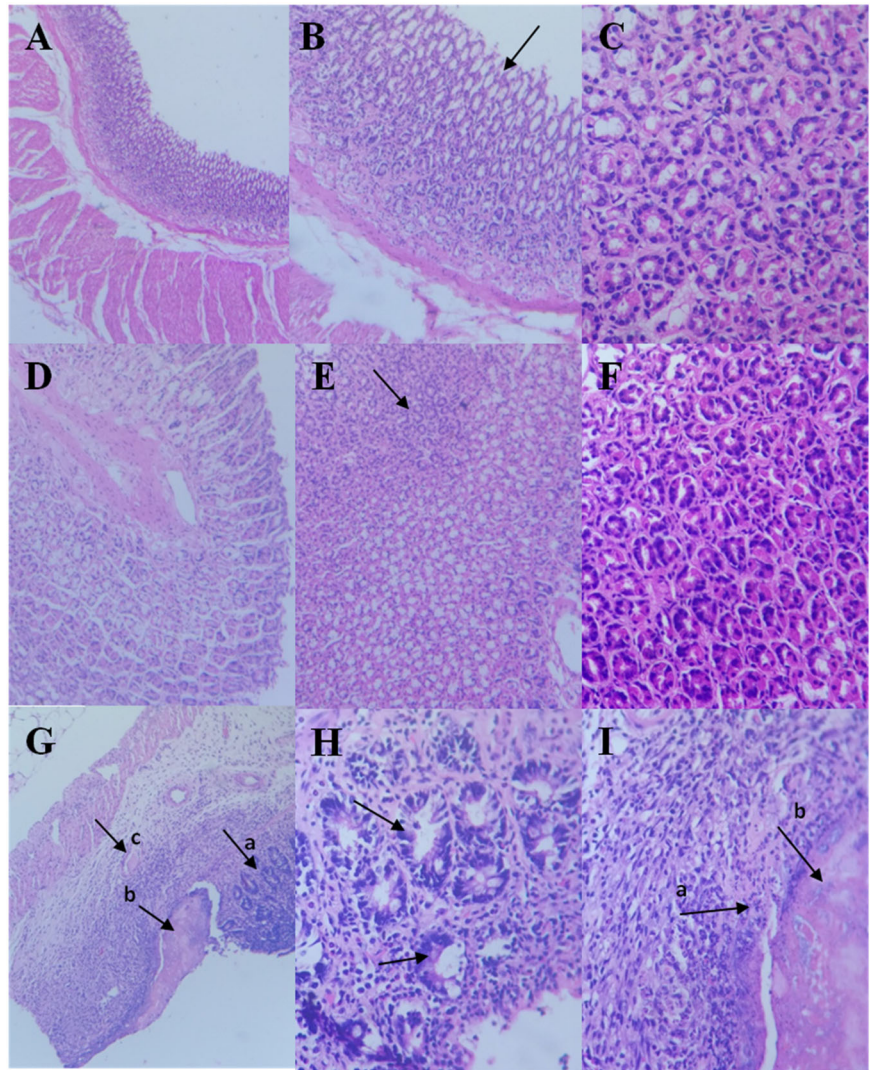


**Fig. 7** PGE<sub>2</sub> and LTB<sub>4</sub> levels after treatment with **7h** in paw tissues at 6 h following carrageenan injection. Graph A; PGE<sub>2</sub> concentration following to **7h** and indomethacin pretreatment and Graph B; LTB<sub>4</sub> concentration following to **7h** and indomethacin pretreatment. The Control group was only received saline and the carrageenan group was

not given pretreatment. The values were shown as mean ± SEM (n = 4). ####p < 0.001 carrageenan group in comparison to control group. \*p < 0.05, \*\*p < 0.01, and \*\*\*p < 0.001 treated group in comparison with carrageenan alone group

**Fig. 8** Gene expression studies on COX-1, COX-2, and 5-LOX enzymes induced by carrageenan after 7h treatment, internal control, GAPDH. Relative gene expression of COX-1, COX-2, and 5-LOX was calculated regarding control samples treated with saline alone indicated by \* $p < 0.05$ . Triplicate experiments were performed and values were expressed as the mean  $\pm$  SEM (graph is generated using CFX Maestro software, Bio-Rad, USA)

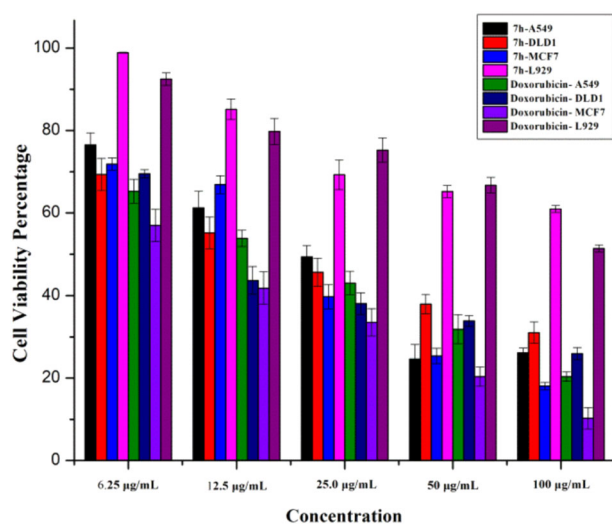
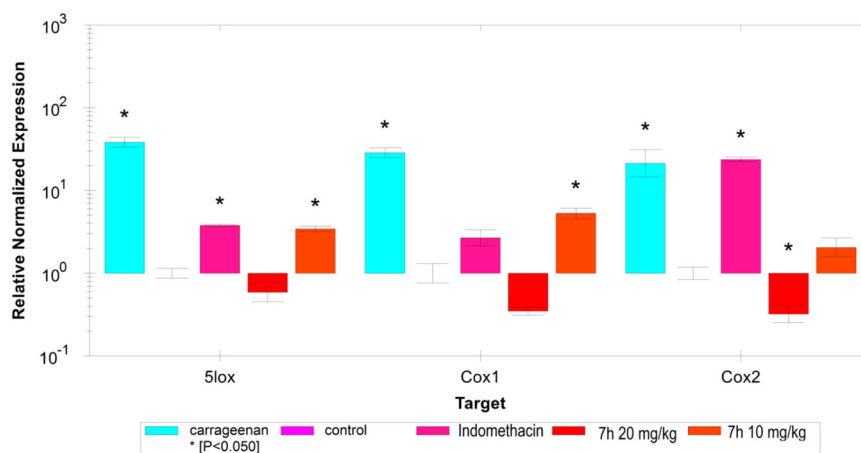


**Fig. 9** Effect of compound **7h** on the percentage of cell viability on the MTT assay. All the results are expressed as mean  $\pm$  SD

SER581, respectively. At COX-2 active site, the compound **7h** demonstrated the best binding conformation with the binding energy of  $-8.87$  Kcal/mol. The diphenyl group of **7h** was surrounded by GLN354, TYR355, GLN350, HIS351, and SER581. Docking simulations of compound **7h** at 5-LOX active site afforded the binding energy of  $-6.68$  Kcal/mol, which was better than reference drug zileuton ( $-6.43$  Kcal/mol). Oxygen atoms of the carbonyl group and the nitro group established hydrogen bonds with TRP147 and ARG 411, respectively. Naphthoyl group was found to have van der Waals interaction, pi-anion, and pi-alkyl interaction with the active site. The binding interaction of **7h** at active sites of COX-2 and 5-LOX is shown in Fig. 11.

## Materials and methods

### Chemistry

All the reagents and solvents were obtained from commercial vendors and used without further purification. Reaction progress was monitored by thin-layer chromatography on pre-coated silica gel 60 F<sub>254</sub> plates (Merck) and chromatogram visualization using the iodine chamber and UV light. Melting points were determined on the Guna Melting point apparatus and were uncorrected. FTIR spectra were obtained using ATR-FTIR Jasco-4100. <sup>1</sup>H and <sup>13</sup>C NMR spectra were recorded on Bruker advance DMX 400-MHz NMR spectrometer at 400 and 100 MHz, respectively, using DMSO-d<sub>6</sub> and CdCl<sub>3</sub> as solvents with internal reference tetramethylsilane. In NMR spectra, chemical shifts ( $\delta$ ) are given in ppm, and coupling constants (J) are expressed in hertz (Hz). High-resolution mass spectra were obtained with JOEL HR mass spectrometer. The purity of final products was analyzed by UPLC-PDA equipped with a pump quaternary solvent manager autosampler-sample manager FTN, and PDA-E-LAMBDA detector. The analytical column used was Acquity UPLC BEH C 18 (150  $\times$  2.1 mm i.d., 130 Å, 1.7  $\mu$ m) at 37 °C. All the compounds showed purity >95%. The elemental analysis was performed on Perkin Elmer 2400 CHNS analyzer and values within  $\pm 0.4\%$  of the calculated values.

### General procedure for compounds 5a–c

To a mixture of an aqueous solution of potassium thiocyanate (1.6 mmol) and TBAF, naphthoyl-1-chloride in 10-mL toluene was added slowly, stirred for 1 h at RT, and then the organic layer was separated. Aromatic or

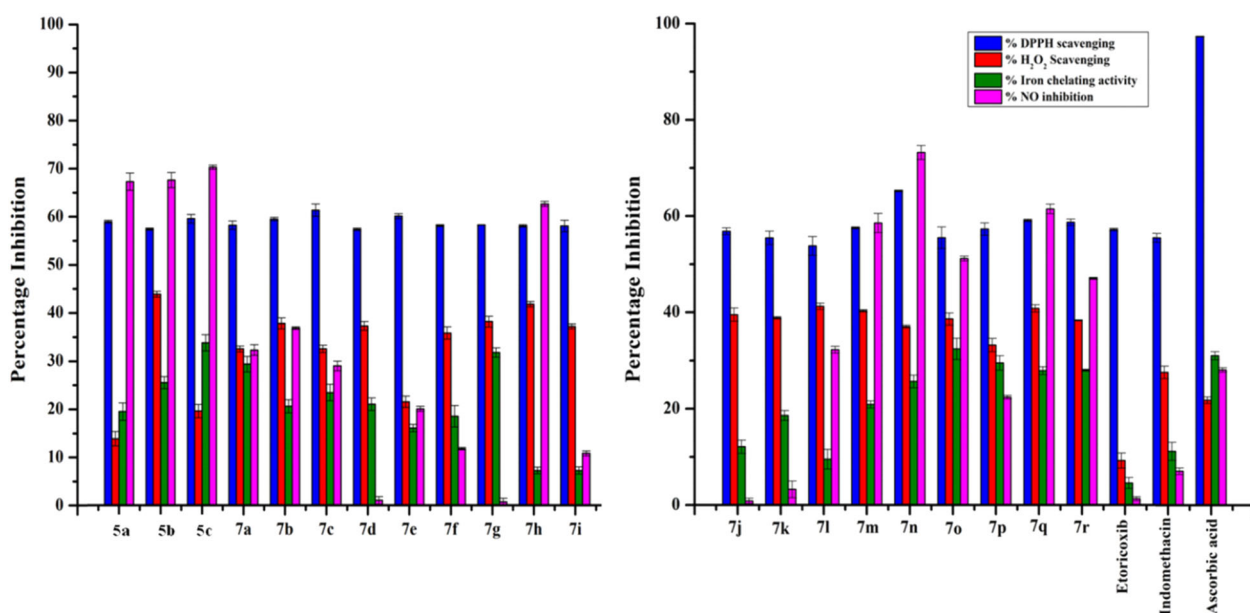
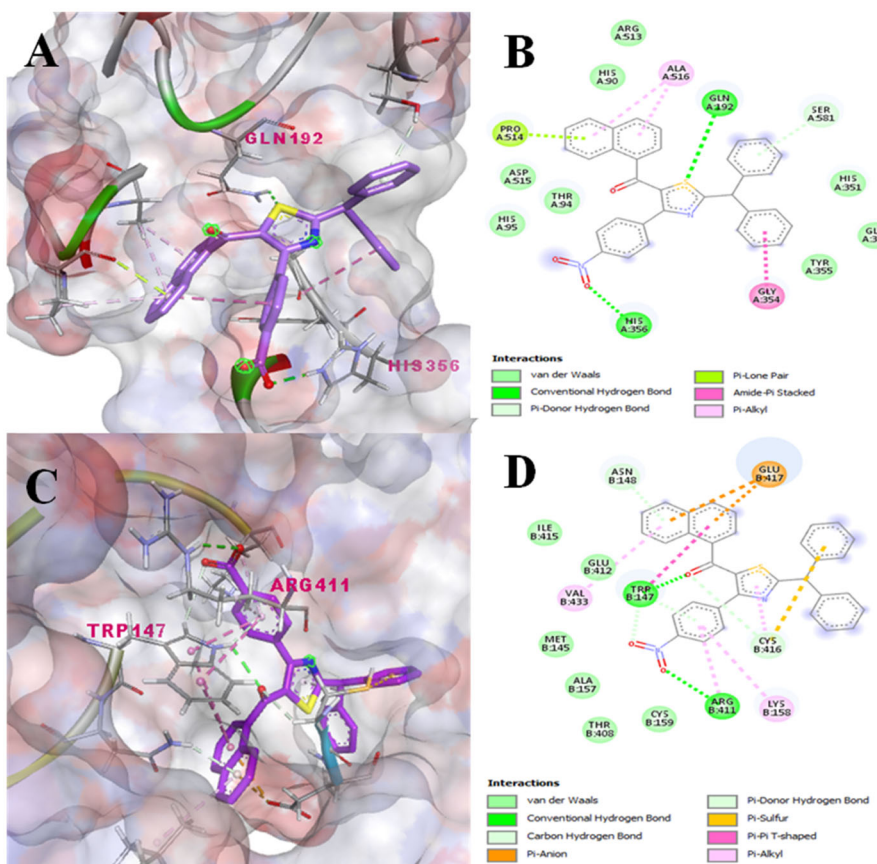


**Fig. 10** Antioxidant activity of compounds **5a–c** and **7a–r** on DPPH scavenging, H<sub>2</sub>O<sub>2</sub> scavenging, iron-chelating activity, and NO scavenging

**Fig. 11** Molecular docking study of compound **7h** at COX-2 (pdb ID 5IKT) and 5-LOX (pdb ID 3O8Y) active sites, **A** 3-D docking conformation of compound **7h** at the active site of COX-2, **B** 2-D illustration at active site of COX-2, **C** 3-D docking conformation of compound **7h** at the active site of 5-LOX, **D** 2-D illustration at the active site of 5-LOX. H-bonds are represented by dashed green lines. Colors depicted are Ligand: purple, oxygen: red, nitrogen: blue, sulfur: yellow. Images are created using Discovery Studio Visualizer



alkylamines (1.5 mmol) were added to the aromatic layer and continued the stirring for 30–60 min or until the reaction completion (monitored by TLC). The separated solid was filtered and recrystallized from ethanol/ethyl acetate.

#### N-(morpholine-4-carbonothioyl)-1-naphthamide (**5a**)

Off-white solid, 88%, mp 154–156 °C. IR (KBr, cm<sup>-1</sup>) 3334 (NH), 1649 (C=O). <sup>1</sup>H NMR (400 MHz, DMSO-d<sub>6</sub>) δ: 3.75

(s, 6H, morpholine-H), 4.19 (s, 2H, morpholine-H), 7.56–7.64 (m, 3H, Ar-H), 7.79 (d,  $J = 6.8$  Hz, 1H, Ar-H), 8.01 (d,  $J = 7.2$  Hz 1H, Ar-H), 8.09 (d,  $J = 8.0$  Hz 1H, Ar-H), 8.24 (d,  $J = 8.0$  Hz 1H, Ar-H), 11.10 (s, 1H, NH).  $^{13}\text{C}$  NMR (100 MHz, DMSO- $d_6$ )  $\delta$ : 50.8, 51.6, 66.2, 125.3, 125.4, 126.9, 127.3, 127.7, 128.9, 130.2, 131.6, 132.4, 133.6, 166.2, 179.8. ESI-MS  $m/z$  for  $\text{C}_{16}\text{H}_{16}\text{N}_2\text{O}_2\text{S}$  [M + H] calcd 301.0932, found 301. Elemental analysis (%) calcd for  $\text{C}_{16}\text{H}_{16}\text{N}_2\text{O}_2\text{S}$  C, 63.98; H, 5.37; N, 9.33; S, 10.67; found: C 63.94, H 5.37, N 9.21, S 10.39.

#### N-(diphenylcarbamothioyl)-1-naphthamide (5b)

Yellow solid, 90%, mp 144–146 °C. IR (KBr,  $\text{cm}^{-1}$ ) 3147 (NH), 1695(C=O).  $^1\text{H}$  NMR (400 MHz,  $\text{CDCl}_3$ )  $\delta$ : 7.27–7.29 (m, 2H, Ar-H), 7.37–7.42 (m, 9H, Ar-H), 7.47–7.50 (m, 3H, Ar-H), 7.81 (d,  $J = 9.28$  Hz, 1H, Ar-H), 7.91 (t,  $J = 7.96$  Hz, 2H, Ar-H), 8.60 (s, 1H, NH).  $^{13}\text{C}$  NMR (100 MHz,  $\text{CDCl}_3$ )  $\delta$ : 124.4, 125.1, 125.9, 126.8, 127.0, 127.6, 127.6, 128.3, 129.3, 130.1, 131.5, 132.3, 133.7, 145.9, 163.4, 182.3. ESI-MS  $m/z$  for  $\text{C}_{24}\text{H}_{18}\text{N}_2\text{OS}$  [M + H] calcd 383.1140, found 383. Elemental analysis (%) calcd for  $\text{C}_{24}\text{H}_{18}\text{N}_2\text{OS}$  C, 75.37; H, 4.74; N, 7.32; S, 8.38 found: C 75.38, H 4.72, N 7.29, S 8.32.

#### N-(phenylcarbamothioyl)-1-naphthamide (5c)

White solid, 90%, mp 184–186 °C. IR (KBr,  $\text{cm}^{-1}$ ) 3159 (NH), 1660 (C=O).  $^1\text{H}$  NMR (400 MHz,  $\text{CDCl}_3$ )  $\delta$ : 7.29 (t,  $J = 7.36$  Hz, 1H, Ar-H), 7.43 (t,  $J = 7.8$  Hz, 2H, Ar-H), 7.51 (t,  $J = 7.68$  Hz, 1H, Ar-H), 7.58 (t,  $J = 7.08$  Hz, 1H, Ar-H), 7.64 (t,  $J = 8.08$  Hz, 1H, Ar-H), 7.76 (d,  $J = 7.96$  Hz, 2H, Ar-H), 7.81 (d,  $J = 7.08$  Hz, 1H, Ar-H), 7.92 (d,  $J = 8.04$  Hz, 1H), 8.04 (d,  $J = 8.24$  Hz, 1H, Ar-H), 8.38 (d,  $J = 8.44$  Hz, 1H, Ar-H), 9.12 (s, 1H, NH), 12.60 (s, 1H, NH).  $^{13}\text{C}$  NMR (100 MHz,  $\text{CDCl}_3$ )  $\delta$ : 124.2, 124.6, 124.6, 126.4, 127.0, 127.1, 128.3, 128.8, 129.0, 129.9, 130.7, 133.2, 133.8, 137.6, 169.2, 178.4. ESI-MS  $m/z$  for  $\text{C}_{18}\text{H}_{14}\text{N}_2\text{OS}$  [M + H] calcd 307.0827, found 307. Elemental analysis (%) calcd for  $\text{C}_{18}\text{H}_{14}\text{N}_2\text{OS}$ , C, 70.56; H, 4.61; N, 9.14; S, 10.46 found: C 70.50, H 4.60, N 8.97, S 10.39.

#### General procedure for the preparation of compound 7a–r

compounds were prepared as illustrated in Scheme 2. 0.1-mol equivalents of TBAF.3H<sub>2</sub>O was added to a mixture of 1.0 mmol of N-naphthoylthiourea (5a–c) and 1.0 mmol of phenacyl bromide (6a–f) in an RB flask charged with a magnetic stirring bar. The resulted reaction mixture was stirred at 80 °C in an oil bath for 1.5 h until the reaction completion and concentrated under reduced pressure.

Desired compounds are afforded by the purification of the residue by column chromatography (hexane/ethyl acetate 10:1 to 20:1).

#### (2-Morpholino-4-phenylthiazol-5-yl)(naphthalen-1-yl)methanone (7a)

Yellow solid, 94%, mp 150–152 °C. IR (KBr,  $\text{cm}^{-1}$ ) 1728 (C=O).  $^1\text{H}$  NMR (400 MHz,  $\text{CDCl}_3$ )  $\delta$ : 3.66 (t,  $J = 4.56$  Hz, 4H, morpholine-H), 3.83 (t,  $J = 5.08$  Hz, 4H, morpholine-H), 6.75 (t,  $J = 7.68$  Hz, 2H, Ar-H), 6.92 (t,  $J = 7.4$  Hz, 1H, Ar-H), 7.01–7.07 (m, 3H, Ar-H), 7.27 (d,  $J = 7.0$  Hz, 1H, Ar-H), 7.42–7.51 (m, 2H, Ar-H), 7.61 (d,  $J = 8.2$  Hz, 1H, Ar-H), 7.70 (d,  $J = 8.0$  Hz, 1H, Ar-H), 8.13 (d,  $J = 8.28$  Hz, 1H, Ar-H).  $^{13}\text{C}$  NMR (100 MHz,  $\text{CDCl}_3$ )  $\delta$ : 48.1, 66.1, 124.0, 125.2, 125.4, 126.0, 127.0, 127.2, 128.1, 128.4, 130.5, 130.7, 133.3, 134.6, 136.5, 160.8, 172.3, 189.3. HRMS (ESI-MS)  $m/z$  for  $\text{C}_{24}\text{H}_{20}\text{N}_2\text{O}_2\text{S}$  [M + H] calcd 401.1245, found 401.1242. Elemental analysis (%) calcd for  $\text{C}_{24}\text{H}_{20}\text{N}_2\text{O}_2\text{S}$  C, 71.98; H, 5.03; N, 6.99; S, 8.01; found: C 71.64, H 5.13, N 6.71, S 7.77.

#### (2-Morpholino-4-(4-nitrophenyl)thiazol-5-yl)(naphthalen-1-yl)methanone (7b)

Fluorescent-yellow solid, 89%, mp 158–160 °C. IR (KBr,  $\text{cm}^{-1}$ ) 1610 (C=O).  $^1\text{H}$  NMR (400 MHz,  $\text{CDCl}_3$ )  $\delta$ : 3.68 (t,  $J = 4.6$  Hz, 4H, morpholine-H), 3.86 (t,  $J = 5.08$  Hz, 4H, morpholine-H), 7.12 (t,  $J = 7.52$  Hz, 1H, Ar-H), 7.20 (d,  $J = 8.68$  Hz, 2H, Ar-H), 7.36 (d,  $J = 6.8$  Hz, 1H, Ar-H), 7.46–7.53 (m, 2H, Ar-H), 7.61 (d,  $J = 8.68$  Hz, 2H, Ar-H), 7.68–7.74 (m, 2H, Ar-H), 8.05 (d,  $J = 8.08$  Hz, 1H, Ar-H).  $^{13}\text{C}$  NMR (100 MHz,  $\text{CDCl}_3$ )  $\delta$ : 48.1, 66.0, 122.0, 124.2, 124.9, 126.4, 126.6, 127.2, 127.3, 128.3, 129.7, 130.5, 131.0, 133.2, 136.5, 140.8, 147.1, 157.6, 172.4, 188.5. HRMS (ESI-MS)  $m/z$  for  $\text{C}_{24}\text{H}_{19}\text{N}_3\text{O}_4\text{S}$  [M + H] calcd 446.1096, found 446.1089. Elemental analysis (%) calcd for  $\text{C}_{24}\text{H}_{19}\text{N}_3\text{O}_4\text{S}$  C, 64.71; H, 4.30; N, 9.43; S, 7.20; found: C 64.40, H 4.07, N 9.21, S 7.07.

#### (4-(4-Fluorophenyl)-2-morpholinothiazol-5-yl)(naphthalen-1-yl)methanone (7c)

Yellow solid, 72%, mp 118–120 °C. IR (KBr,  $\text{cm}^{-1}$ ) 1734 (C=O).  $^1\text{H}$  NMR (400 MHz,  $\text{CDCl}_3$ )  $\delta$ : 3.65 (t,  $J = 4.6$  Hz, 4H, morpholine-H), 3.82 (t,  $J = 5.12$  Hz, 4H, morpholine-H), 6.95 (d,  $J = 8.12$  Hz, 2H, Ar-H), 7.06–7.11 (m, 3H, Ar-H), 7.29 (d,  $J = 8.0$  Hz, 1H, Ar-H), 7.41–7.48 (m, 2H, Ar-H), 7.62 (d,  $J = 8.2$  Hz, 1H, Ar-H), 7.68 (d,  $J = 7.36$ , 1H, Ar-H), 7.99 (d,  $J = 7.76$  Hz, 1H, Ar-H).  $^{13}\text{C}$  NMR (100 MHz,  $\text{CDCl}_3$ )  $\delta$ : 48.1, 66.0, 123.7, 124.2, 124.9, 126.2, 126.2, 127.0, 127.1, 128.3, 129.0, 130.5, 130.8, 133.2, 136.5, 137.9, 159.0, 172.5, 188.9. HRMS (ESI-MS)

$m/z$  for  $C_{24}H_{19}FN_2O_2S$  [M + H] calcd 419.1151, found 419.1148. Elemental analysis (%) calcd for  $C_{24}H_{19}FN_2O_2S$  C, 68.88; H, 4.58; N, 6.69; S, 7.66; found: C 68.69, H 4.21, N 6.26, S 7.49.

**(2-Morpholino-4-(4-(trifluoromethyl)phenyl)thiazol-5-yl)(naphthalen-1-yl)methanone (7d)**

Yellow solid, 89%, mp 170–172 °C. IR (KBr,  $cm^{-1}$ ) 1701 (C=O).  $^1H$  NMR (400 MHz,  $CDCl_3$ )  $\delta$ : 3.66 (t,  $J = 4.52$  Hz, 4H, morpholine-H), 3.84 (t,  $J = 5.04$  Hz, 4H, morpholine-H), 6.95 (d,  $J = 8.16$  Hz, 2H, Ar-H), 7.06 (t,  $J = 8.28$  Hz, 3H, Ar-H), 7.29 (d,  $J = 6.96$  Hz, 1H, Ar-H), 7.41–7.48 (m,  $J = 7.0$  Hz, 2H, Ar-H), 7.62 (d,  $J = 8.2$  Hz, 1H, Ar-H), 7.68 (d,  $J = 8.68$  Hz, 1H, Ar-H), 7.99 (d,  $J = 8.12$  Hz, 1H, Ar-H).  $^{13}C$  NMR (100 MHz,  $CDCl_3$ )  $\delta$ : 48.1, 66.0, 123.7, 124.1, 124.9, 126.2, 126.2, 127.0, 127.1, 128.3, 129.0, 130.5, 130.8, 133.2, 136.5, 137.9, 159.0, 172.5, 189.9. HRMS (ESI-MS)  $m/z$  for  $C_{25}H_{19}F_3N_2O_2S$  [M + H] calcd 469.1119, found 469.1115. Elemental analysis (%) calcd for  $C_{25}H_{19}F_3N_2O_2S$  C, 64.09; H, 4.09; N, 5.98; S, 6.84; found: C 63.99, H 4.01, N 5.75, S 6.72.

**4-(5-(1-Naphthoyl)-2-morpholinothiazol-4-yl)benzotrile (7e)**

Pale-yellow solid, 87%, mp 202–204 °C. IR (KBr,  $cm^{-1}$ ) 2223 (CN), 1697 (C=O).  $^1H$  NMR (400 MHz,  $CDCl_3$ )  $\delta$ : 3.65 (t,  $J = 4.6$  Hz, 4H, morpholine-H), 3.83 (t,  $J = 5.08$  Hz, 4H, morpholine-H), 7.04 (d,  $J = 8.28$  Hz, 2H, Ar-H), 7.10–7.16 (m, 3H, Ar-H), 7.32 (d,  $J = 6.88$  Hz, 1H, Ar-H), 7.46–7.52 (m, 2H, Ar-H), 7.71 (d,  $J = 8.2$  Hz, 1H, Ar-H), 7.76 (d,  $J = 7.04$  Hz, 1H, Ar-H), 8.04 (d,  $J = 7.56$  Hz, 1H, Ar-H).  $^{13}C$  NMR (100 MHz,  $CDCl_3$ )  $\delta$ : 48.2, 66.1, 113.4, 118.1, 124.5, 125.3, 125.7, 126.1, 126.8, 127.8, 128.2, 128.8, 129.6, 130.4, 131.8, 132.3, 133.2, 142.0, 159.9, 172.8, 187.2. HRMS (ESI-MS)  $m/z$  for  $C_{25}H_{19}N_3O_2S$  [M + H] calcd 426.1198, found 426.1196. Elemental analysis (%) calcd for  $C_{25}H_{19}N_3O_2S$  C, 70.57; H, 4.50; N, 9.88; S, 7.53; found: C 70.24, H 4.38, N 9.64, S 7.37.

**(2-Morpholino-4-(4-methylphenyl)thiazol-5-yl)(naphthalen-1-yl)methanone (7f)**

Pale-yellow solid, 77%, mp 138–140 °C. IR (KBr,  $cm^{-1}$ ) 1608 (C=O).  $^1H$  NMR (400 MHz,  $CDCl_3$ )  $\delta$ : 2.09 (s, 3H,  $CH_3$ ), 3.65 (t,  $J = 4.52$  Hz, 4H, morpholine-H), 3.83 (t,  $J = 4.64$  Hz, 4H, morpholine-H), 6.55 (d,  $J = 7.64$  Hz, 2H, Ar-H), 6.97 (d,  $J = 7.72$  Hz, 2H, Ar-H), 7.04 (t,  $J = 7.64$  Hz, 1H, Ar-H), 7.29 (d,  $J = 6.92$  Hz, 1H, Ar-H), 7.42–7.50 (m, 2H, Ar-H), 7.64 (d,  $J = 8.08$  Hz, 1H, Ar-H), 7.71 (d,  $J = 7.52$  Hz, 1H, Ar-H), 8.12 (d,  $J = 8.0$  Hz, 1H, Ar-H).  $^{13}C$  NMR (100 MHz,  $DMSO-d_6$ )  $\delta$ : 21.1, 48.1, 66.1, 124.1,

124.9, 125.3, 126.0, 126.9, 127.1, 127.7, 128.0, 128.9, 130.2, 130.7, 131.7, 133.4, 136.8, 138.4, 160.9, 172.2, 189.2. HRMS (ESI-MS)  $m/z$  for  $C_{25}H_{22}N_2O_2S$  [M + H] calcd 415.1402, found 415.1400. Elemental analysis (%) calcd for  $C_{25}H_{22}N_2O_2S$  C, 72.44; H, 5.35; N, 6.76; S, 7.73; found: C 72.07, H 5.16, N 6.53, S 7.56.

**(2-(Diphenylamino)-4-phenylthiazol-5-yl)(naphthalen-1-yl)methanone (7g)**

Pale-yellow solid, 78%, mp 150–152 °C. IR (KBr,  $cm^{-1}$ ) 1602 (C=O).  $^1H$  NMR (400 MHz,  $CDCl_3$ )  $\delta$ : 6.75 (t,  $J = 7.6$  Hz, 2H, Ar-H), 6.92 (t,  $J = 7.36$  Hz, 1H, Ar-H), 7.03 (t,  $J = 7.48$  Hz, 1H, Ar-H), 7.12 (d,  $J = 7.2$ , 2H, Ar-H), 7.30–7.37 (m, 3H, Ar-H), 7.43 (t,  $J = 8.08$ , 5H, Ar-H), 7.50–7.56 (m, 5H, Ar-H), 7.65 (d,  $J = 8.16$  Hz, 1H, Ar-H), 7.74 (d,  $J = 8.16$  Hz, 1H, Ar-H), 8.22 (d,  $J = 8.4$  Hz, 1H, Ar-H).  $^{13}C$  NMR (100 MHz,  $CDCl_3$ )  $\delta$ : 124.0, 125.2, 126.1, 126.3, 127.0, 127.1, 127.2, 127.6, 128.2, 128.4, 129.2, 129.8, 130.8, 130.9, 133.4, 134.6, 136.3, 144.1, 159.8, 171.3, 189.7. HRMS (ESI-MS)  $m/z$  for  $C_{32}H_{22}N_2OS$  [M + H] calcd 483.1453, found 483.1449. Elemental analysis (%) calcd for  $C_{32}H_{22}N_2OS$  C, 79.64; H, 4.60; N, 5.80; S, 6.64; found: C 79.35, H 4.18, N 5.53, S 6.51.

**(2-(Diphenylamino)-4-(4-nitrophenyl)thiazol-5-yl)(naphthalen-1-yl)methanone (7h)**

Flourescent yellow solid, 89%, mp 230–232 °C. IR (KBr,  $cm^{-1}$ ) 1715 (C=O).  $^1H$  NMR (400 MHz,  $CDCl_3$ )  $\delta$ : 7.10 (t,  $J = 7.8$  Hz, 1H, Ar-H), 7.26 (d,  $J = 6.72$  Hz, 2H, Ar-H), 7.32 (t,  $J = 7.08$  Hz, 2H, Ar-H), 7.40 (d,  $J = 7.04$ , 1H, Ar-H), 7.44–7.54 (m, 10H, Ar-H), 7.61 (d,  $J = 8.76$ , 2H, Ar-H), 7.69 (d,  $J = 8.24$ , 1H, Ar-H), 7.73 (d,  $J = 7.72$ , 1H, Ar-H), 8.11 (d,  $J = 8.32$  Hz, 1H, Ar-H).  $^{13}C$  NMR (100 MHz,  $CDCl_3$ )  $\delta$ : 122.0, 124.1, 124.8, 126.2, 126.5, 127.4, 127.5, 127.6, 128.1, 128.3, 129.9, 129.9, 130.5, 131.3, 133.3, 136.2, 140.7, 143.8, 147.1, 156.6, 171.6, 188.9. HRMS (ESI-MS)  $m/z$  for  $C_{32}H_{21}N_3O_3S$  [M + H] calcd 528.1304, found 528.1301. Elemental analysis (%) calcd for  $C_{32}H_{21}N_3O_3S$  C, 72.85; H, 4.01; N, 7.96; S, 6.08; found: C 72.66, H 3.83, N 7.68, S 5.79.

**(2-(Diphenylamino)-4-(4-fluorophenyl)thiazol-5-yl)(naphthalen-1-yl)methanone (7i)**

Yellow solid, 72%, mp 162–164 °C. IR (KBr,  $cm^{-1}$ ) 1732 (C=O).  $^1H$  NMR (400 MHz,  $CDCl_3$ )  $\delta$ : 6.44 (t,  $J = 8.68$  Hz, 2H, Ar-H), 7.09 (t,  $J = 7.56$  Hz, 3H, Ar-H), 7.30–7.38 (m, 3H, Ar-H), 7.43–7.53 (m, 10H, Ar-H), 7.71 (d,  $J = 8.2$ , 1H, Ar-H), 7.76 (d,  $J = 7.8$ , 1H, Ar-H), 8.16 (d,  $J = 8.28$  Hz, 1H, Ar-H).  $^{13}C$  NMR (100 MHz,  $CDCl_3$ )  $\delta$ : 113.9, 114.1, 124.1, 125.1, 126.2, 126.3, 126.8, 127.1,

127.2, 127.5, 128.3, 129.8, 130.6, 130.7, 130.9, 131.0, 131.1, 133.4, 136.3, 144.0, 158.6, 161.3, 163.8, 171.3, 189.4, 171.3, 189.4. HRMS (ESI-MS)  $m/z$  for  $C_{32}H_{21}FN_2OS$  [M + H] calcd 501.1359, found 501.1354. Elemental analysis (%) calcd for  $C_{32}H_{21}FN_2OS$  C 76.78; H, 4.23; N, 5.60; S, 6.40; found: C 76.61, H 3.94, N 5.36, S 6.07.

**(2-(Diphenylamino)-4-(4-(trifluoromethyl)phenyl)thiazol-5-yl)(naphthalen-1-yl)methanone (7j)**

Yellow solid, 84%, mp 178–180 °C. IR (KBr,  $cm^{-1}$ ) 1697 (C=O).  $^1H$  NMR (400 MHz,  $CDCl_3$ )  $\delta$ : 6.98 (d,  $J$  = 8.08 Hz, 2H, Ar-H), 7.08 (t,  $J$  = 7.4 Hz, 1H, Ar-H), 7.14 (d,  $J$  = 8.04 Hz, 2H, Ar-H), 7.31–7.37 (m, 3H, Ar-H), 7.43–7.52 (m, 10H, Ar-H), 7.66 (d,  $J$  = 8.2 Hz, 1H, Ar-H), 7.71 (d,  $J$  = 8.04 Hz, 1H, Ar-H), 8.08 (d,  $J$  = 8.24 Hz, 1H, Ar-H).  $^{13}C$  NMR (100 MHz,  $CDCl_3$ )  $\delta$ : 123.7, 123.7, 124.1, 124.9, 126.2, 126.3, 127.2, 127.3, 127.4, 127.7, 128.3, 129.2, 129.9, 130.5, 131.1, 133.3, 136.2, 137.9, 143.9, 158.1, 171.6, 189.2. HRMS (ESI-MS)  $m/z$  for  $C_{33}H_{21}F_3N_2OS$  [M + H] calcd 551.1327, found 551.1324. Elemental analysis (%) calcd for  $C_{33}H_{21}F_3N_2OS$  C, 71.99; H, 3.84; N, 5.09; S, 5.82; found: C 71.68, H 3.57, N 4.93, S 5.72.

**4-(5-(1-Naphthoyl)-2-(diphenylamino)thiazol-4-yl)benzoxazole (7k)**

Bright-yellow solid, 90%, mp 190–192 °C. IR (KBr,  $cm^{-1}$ ) 2227 (CN), 1602 (C=O).  $^1H$  NMR (400 MHz,  $CDCl_3$ )  $\delta$ : 7.04 (d,  $J$  = 8.36 Hz, 2H, Ar-H), 7.10 (t,  $J$  = 7.92 Hz, 1H, Ar-H), 7.18 (d,  $J$  = 8.32 Hz, 2H, Ar-H), 7.32–7.39 (m, 3H, Ar-H), 7.44–7.54 (m, 10H, Ar-H), 7.73 (d,  $J$  = 8.24, 1H, Ar-H), 7.77 (d,  $J$  = 7.48 Hz, 1H, Ar-H), 8.12 (d,  $J$  = 8.16 Hz, 1H, Ar-H).  $^{13}C$  NMR (100 MHz,  $CDCl_3$ )  $\delta$ : 111.6, 118.5, 124.1, 124.9, 126.2, 126.4, 127.3, 127.5, 127.6, 127.9, 128.4, 129.6, 129.9, 130.6, 131.3, 133.3, 136.1, 138.9, 143.9, 157.1, 171.6, 188.9. HRMS (ESI-MS)  $m/z$  for  $C_{33}H_{21}N_3OS$  [M + H] calcd 508.1405, found 508.1403. Elemental analysis (%) calcd for  $C_{33}H_{21}N_3OS$  C, 78.08; H, 4.17; N, 8.28; S, 6.32; found: C 77.75, H 4.06, N 8.01, S 6.14.

**(2-(Diphenylamino)-4-(4-methylphenyl)thiazol-5-yl)(naphthalen-1-yl)methanone (7l)**

Pale-yellow solid, 88%, mp 220–222 °C. IR (KBr,  $cm^{-1}$ ) 1697 (C=O).  $^1H$  NMR (400 MHz,  $CDCl_3$ )  $\delta$ : 2.11 (s, 3H,  $CH_3$ ), 6.58 (d,  $J$  = 7.88 Hz, 2H, Ar-H), 7.04 (d,  $J$  = 7.96 Hz, 2H, Ar-H), 7.08 (d,  $J$  = 8.12 Hz, 1H, Ar-H), 7.29 (t,  $J$  = 7.32 Hz, 2H, Ar-H), 7.37 (d,  $J$  = 6.12 Hz, 1H, Ar-H), 7.42–7.53 (m, 10H, Ar-H), 7.68 (d,  $J$  = 8.2 Hz, 1H, Ar-H),

7.75 (d,  $J$  = 7.6 Hz, 1H, Ar-H), 8.21 (d,  $J$  = 8.36 Hz, 1H, Ar-H).  $^{13}C$  NMR (100 MHz,  $CDCl_3$ )  $\delta$ : 21.1, 124.1, 125.3, 126.0, 126.3, 127.0, 127.1, 127.5, 127.7, 128.1, 129.2, 129.8, 130.6, 130.8, 131.7, 133.4, 136.5, 138.4, 160.0, 171.1, 189.6. HRMS (ESI-MS)  $m/z$  for  $C_{33}H_{24}N_2OS$  [M + H] calcd 497.1609, found 497.1601. Elemental analysis (%) calcd for  $C_{33}H_{24}N_2OS$ , C, 79.81; H, 4.87; N, 5.64; S, 6.46 found: C 79.65, H 4.61, N 5.47, S 6.28.

**N-(3,4-diphenylthiazol-2(3H)-ylidene)-1-naphthamide (7m)**

Pale-yellow solid, 82%, mp 198–200 °C. IR (KBr,  $cm^{-1}$ ) 3425 (NH), 1610 (C=O).  $^1H$  NMR (400 MHz,  $CDCl_3$ )  $\delta$ : 6.74 (s, 1H, N-H), 7.14 (d,  $J$  = 6.72 Hz, 2H, Ar-H), 7.22–7.31 (m, 5H, Ar-H), 7.37–7.44 (m, 6H, Ar-H), 7.80 (t,  $J$  = 5.16 Hz, 1H, Ar-H), 7.87 (d,  $J$  = 8.12 Hz, 1H, Ar-H), 8.28 (d,  $J$  = 7.28 Hz, 1H, Ar-H), 9.22 (t,  $J$  = 9.84 Hz, 1H, Ar-H).  $^{13}C$  NMR (100 MHz,  $CDCl_3$ )  $\delta$ : 107.4, 124.7, 125.5, 126.6, 127.2, 128.2, 128.4, 128.6, 128.8, 129.0, 130.4, 130.6, 131.9, 132.0, 133.5, 134.0, 137.9, 139.1, 169.6, 176.4. HRMS (ESI-MS)  $m/z$  for  $C_{26}H_{18}N_2OS$  [M + H] calcd 407.1140, found 407.1137. Elemental analysis (%) calcd for  $C_{26}H_{18}N_2OS$ , C, 76.82; H, 4.46; N, 6.89; S, 7.89 found: C 76.42, H 3.89, N 6.26, S 7.69.

**N-(4-(4-nitrophenyl)-3-phenylthiazol-2(3H)-ylidene)-1-naphthamide (7n)**

Bright-yellow solid, 86%, mp 212–214 °C. IR (KBr,  $cm^{-1}$ ) 3435 (NH), 3261 (NH), 1773 (C=O).  $^1H$  NMR (400 MHz,  $CDCl_3$ )  $\delta$ : 6.72 (s, 1H, Thiazolidene-H), 6.91 (t,  $J$  = 8.68 Hz, 2H, Ar-H), 7.11–7.15 (m, 2H, Ar-H), 7.27–7.30 (m, 2H, Ar-H), 7.39–7.45 (m, 6H, Ar-H), 7.79 (t,  $J$  = 5.16 Hz, 1H, Ar-H), 7.88 (d,  $J$  = 8.12 Hz, 1H, Ar-H), 8.28 (d,  $J$  = 8.4 Hz, 1H, Ar-H), 9.22 (d,  $J$  = 9.88 Hz, 1H, Ar-H).  $^{13}C$  NMR (100 MHz,  $CDCl_3$ )  $\delta$ : 110.3, 123.7, 124.7, 125.6, 126.9, 127.0, 128.3, 128.4, 129.1, 129.4, 129.5, 130.7, 132.5, 133.0, 134.0, 136.7, 136.8, 137.3, 176.6. HRMS (ESI-MS)  $m/z$  for  $C_{26}H_{17}N_3O_3S$  [M + H] calcd 452.0991, found 452.0989. Elemental analysis (%) calcd for  $C_{26}H_{17}N_3O_3S$ , C, 69.17; H, 3.80; N, 9.31; S, 7.10 found: C 69.11, H 4.00, N 9.19, S 6.98.

**N-(4-(4-fluorophenyl)-3-phenylthiazol-2(3H)-ylidene)-1-naphthamide (7o)**

Off-white solid, 82%, mp 202–204 °C. IR (KBr,  $cm^{-1}$ ) 3159 (NH), 1660 (C=O).  $^1H$  NMR (400 MHz,  $CDCl_3$ )  $\delta$ : 6.74 (s, 1H, N-H), 6.94 (t,  $J$  = 8.68, 2H, Ar-H), 7.14–7.17 (m, 2H, Ar-H), 7.30 (m, 2H, Ar-H), 7.41–7.47 (m, 5H, Ar-H), 7.82 (t,  $J$  = 5.16 Hz, 1H, Ar-H), 7.90 (d,  $J$  = 8.12 Hz, 1H, Ar-H), 8.30 (d,  $J$  = 6.16 Hz, 1H, Ar-H), 9.24 (d,  $J$  = 8.28, 1H, Ar-H),  $^{13}C$  NMR (100 MHz,  $CDCl_3$ )  $\delta$ : 107.5,

115.5, 115.7, 124.7, 125.5, 126.7, 127.1, 128.2, 128.6, 128.7, 129.1, 130.5, 130.8, 130.9, 131.7, 132.1, 133.4, 134.0, 137.7, 138.0, 161.6, 164.1, 169.5, 176.4. HRMS (ESI-MS)  $m/z$  for  $C_{26}H_{17}FN_2OS$  [M + H] calcd 425.1046, found 425.1043. Elemental analysis (%) calcd for  $C_{26}H_{17}FN_2OS$ , C 73.57; H, 4.04; F, 4.48; N, 6.60; S, 7.55 found: C 73.19, H 4.02, N 6.64, S 7.55.

#### N-(3-phenyl-4-(4-(trifluoromethyl)phenyl)thiazol-2(3H)-ylidene)-1-naphthamide (7p)

Pale-yellow solid, 79%, mp 142–144 °C. IR (KBr,  $cm^{-1}$ ) 3340 (NH), 1620 (C=O).  $^1H$  NMR (400 MHz,  $CDCl_3$ )  $\delta$ : 6.82 (s, 1H, N-H), 7.26 (d,  $J = 8.4$  Hz, 2H, Ar-H), 7.31 (d,  $J = 7.92$  Hz, 2H, Ar-H), 7.42–7.51 (m, 8H, Ar-H), 7.84 (t,  $J = 6.0$  Hz, 1H, Ar-H), 7.91 (d,  $J = 8.08$  Hz, 1H, Ar-H), 8.32 (d,  $J = 7.24$  Hz, 1H, Ar-H), 9.27 (t,  $J = 6.0$  Hz, 1H, Ar-H).  $^{13}C$  NMR (100 MHz,  $CDCl_3$ )  $\delta$ : 109.1, 122.4, 124.7, 125.1, 125.4, 125.4, 125.4, 125.5, 125.6, 126.8, 127.0, 128.3, 128.5, 128.9, 129.1, 129.3, 130.6, 130.9, 131.9, 132.3, 133.2, 134.0, 134.0, 137.5, 137.5, 169.5, 176.4. HRMS (ESI-MS)  $m/z$  for  $C_{27}H_{17}F_3N_2OS$  [M + H] calcd 475.1014, found 475.1011. Elemental analysis (%) calcd for  $C_{27}H_{17}F_3N_2OS$ , C, 68.34; H, 3.61; F, 12.01; N, 5.90; S, 6.76 found: C 68.34, H 3.61, N 6.00, S 6.78.

#### N-(4-(4-cyanophenyl)-3-phenylthiazol-2(3H)-ylidene)-1-naphthamide (7q)

Pale-yellow solid, 88%, mp 250–252 °C. IR (KBr,  $cm^{-1}$ ) 3264 (NH), 2227 (CN), 1597 (C=O).  $^1H$  NMR (400 MHz,  $CDCl_3$ )  $\delta$ : 6.85 (s, 1H, N-H), 7.24 (d,  $J = 5.68$  Hz, 2H, Ar-H), 7.28 (d,  $J = 7.92$  Hz, 2H, Ar-H), 7.39–7.45 (m, 5H, Ar-H), 7.51 (d,  $J = 8.32$ , 2H, Ar-H), 7.82 (t,  $J = 6.16$  Hz, 1H, Ar-H), 7.90 (d,  $J = 8.08$  Hz, 1H, Ar-H), 8.28 (d,  $J = 7.28$  Hz, 1H, Ar-H), 9.22 (t,  $J = 6.36$  Hz, 1H, Ar-H).  $^{13}C$  NMR (100 MHz,  $CDCl_3$ )  $\delta$ : 110.7, 111.8, 118.7, 125.3, 126.2, 126.9, 127.2, 128.8, 129.1, 129.5, 129.6, 129.9, 130.3, 131.3, 132.3, 132.6, 133.9, 134.0, 135.3, 137.5, 137.8, 169.6, 175.5. HRMS (ESI-MS)  $m/z$  for  $C_{27}H_{17}N_3OS$  [M + H] calcd 432.1092 found 432.1088. Elemental analysis (%) calcd for  $C_{27}H_{17}N_3OS$ , C, 75.15; H, 3.97; N, 9.74; O, 3.71; S, 7.43 found: C 75.01, H 3.96, N 9.74, S 7.09.

#### N-(3-phenyl-4-(p-methylphenyl)thiazol-2(3H)-ylidene)-1-naphthamide (7r)

Off-white solid, 77%, mp 186–188 °C. IR (KBr,  $cm^{-1}$ ) 3351 (NH), 1651 (C=O).  $^1H$  NMR (400 MHz,  $CDCl_3$ )  $\delta$ : 2.30 (s, 3H,  $CH_3$ ), 6.70 (s, 1H, N-H), 7.03 (s, 3H, Ar-H), 7.29 (d,  $J = 6.52$  Hz, 2H, Ar-H), 7.39–7.43 (m, 6H, Ar-H), 7.80 (t,  $J = 6.8$  Hz, 1H, Ar-H), 7.87 (d,  $J = 8.08$  Hz, 1H, Ar-H), 8.28 (d,  $J = 6.28$  Hz, 1H, Ar-H), 9.22 (d,  $J = 9.76$  Hz, 1H,

Ar-H).  $^{13}C$  NMR (100 MHz,  $CDCl_3$ )  $\delta$ : 21.3, 107.0, 124.7, 125.5, 126.6, 127.2, 127.7, 128.2, 128.5, 128.6, 128.8, 128.97, 129.1, 130.4, 131.9, 132.0, 133.6, 134.0, 137.9, 138.9, 139.2, 169.6, 176.3. HRMS (ESI-MS)  $m/z$  for  $C_{27}H_{20}N_2OS$  [M + H] calcd 421.1296, found 421.1292. Elemental analysis (%) calcd for  $C_{27}H_{20}N_2OS$ , C, 77.12; H, 4.79; N, 6.66; S, 7.62 found: C 77.02, H 4.90, N 6.63, S 7.32.

## Biological activity

### In vitro COX-1 and COX-2 inhibitory assay

The COX-1 and COX-2 inhibitory activities of the synthesized compounds were screened by human COX-1 (Catalog no. 701070) and human COX-2 recombinant inhibitor screening assay (Catalog no. 701080) provided by Cayman chemical, USA according to manufacturer's instructions. In this assay,  $SnCl_2$  reduces COX-derived  $PGH_2$  to  $PGF_2\alpha$  and is measured directly. COX-1/COX-2 100% initial activity tubes contained 160  $\mu$ L of reaction buffer, 10- $\mu$ L heme, and 10- $\mu$ L COX-1/COX-2 enzymes in respective tubes. Also, enzyme inhibitor tubes consisted of 10  $\mu$ L of inhibitor (inhibitors were added at 0.01, 0.1, 1.0, 10, and 100  $\mu$ M final concentration) in each tube in addition to the above components. The background tubes correspond to inactivated enzymes. After incubation of the tubes for 10 min at 37 °C, 10  $\mu$ L of AA was added to each tube to initiate the reactions and continued the incubation for another 2 min. The enzyme catalysis was quenched with 30  $\mu$ L of  $SnCl_2$  solution in HCl. The PGs generated in each well was measured by specific PG antiserum. The PGs produced in each well compete with added PG tracer for a limited amount of PG antiserum and the amount of PG tracer that binds to the PG antiserum will be inversely proportional to the concentration of PG in the well. Then Ellman's reagent was added and the color developed was measured spectrophotometrically at 410 nm.  $IC_{50}$  values were determined from percentage inhibition versus concentration of inhibitor. In this study, all the synthesized compounds were subjected to COX-2 screening and selected compounds with potential COX-2 inhibition were further studied for COX-1 inhibitory activity [5].

### In vitro 5-LOX inhibitory assay

For 5-LOX inhibitory assay, samples were screened at 0.01, 0.1, 1.0, 10, 100  $\mu$ M using LOX inhibitor screening assay kits (Catalog no. 760700, Catalog no.60401) provided by Cayman chemical, USA as per manufacturer's directions. The inhibitor well consists of 10- $\mu$ L inhibitor and 90- $\mu$ L 5-LOX enzyme and each concentration was checked in duplicate. After incubation for 5 min at RT, 10- $\mu$ L substrate

(linoleic acid) was added to blank wells (100- $\mu$ l assay buffer), positive control wells (90  $\mu$ l of 5-LOX enzyme and 10- $\mu$ l assay buffer), 100% initial activity wells (90- $\mu$ l 5-LOX enzyme and 10- $\mu$ l inhibitor vehicle), and inhibitor wells. By the addition of chromogen (100  $\mu$ l), enzyme catalysis was stopped and the color was developed. The absorbance was measured at 495-nm spectrophotometrically [32].

#### PGE<sub>2</sub> and LTB<sub>4</sub> screening assay on LPS-induced RAW 264.7 cell lines

PGE<sub>2</sub> and LTB<sub>4</sub> production in LPS-induced RAW 264.7 cells was investigated to determine the anti-inflammatory potency. In short, Raw 264.7 cells were seeded on 96-well plates at a density of  $1 \times 10^4$  cells per well, incubated for 18 h. The cells were subjected to aspirin pretreatment (500  $\mu$ M) for 3 h to inactivate COX-1 activity. The cells were then washed twice with PBS (phosphate buffer solution). In the fresh DMEM with or without LPS (1  $\mu$ g/ml), cells were subsequently pretreated with different concentrations of test and reference compounds (0.1, 1.0, 10.0  $\mu$ M) for 2 h before further 16-h incubation. After incubation, the supernatant was obtained by centrifugation [33]. PGE<sub>2</sub> and LTB<sub>4</sub> produced were determined by the ELISA method using the PGE<sub>2</sub> and leukotriene B<sub>4</sub> parameter kits according to the manufacturer's instruction (Catalog No. KGE004B & KGE006B, R&D Systems, Inc. USA).

#### In vivo biological studies

All in vivo biological studies were carried out with male Wistar rats housed at  $23 \pm 2$  °C in 12-h light/12-h dark cycles with food and water ad libitum in the animal house, Vellore Institute of Technology, Vellore, Tamil Nadu. All the experimental procedures have been duly approved by CPSCEA.

#### Studies for checking toxicity

Male Wistar rats were used to study the acute toxicity of compound **7h** as per OECD guidelines. Briefly, the animals were grouped into four of three animals each and subjected to overnight fasting before dosing and 4 h after dosing. Group I treated with vehicle and served as control. Group II, III, and IV received a single dose of compound **7h** at 50, 500, and 2000 mg/kg, respectively. Animals were monitored constantly during the first 4 h and followed by monitoring at regular intervals for 24 h. Afterward, monitoring was continued once daily for 14 days. After 14 days, animals were sacrificed and gross evaluation of kidney, heart, liver, stomach, and intestine was done by histopathological studies [5].

#### Anti-inflammatory studies

The in vivo anti-inflammatory potency of **7h** and reference drug indomethacin was determined using the carrageenan-induced rat-paw edema model as per previous reports [34, 35]. Male Wistar rats of weight 150–180 g were randomly grouped into four, each comprising five animals. Group I, negative control, received vehicle. Group II, positive control, administered with indomethacin 10 mg/kg. Group III and group IV received **7h** at 10, and 20-mg/kg doses respectively. Both test and reference compounds were suspended normal saline with the aid of 0.1% w/v CMC-Na and administered orally. Edema was induced 1 h after drug administration by sub-plantar injection of freshly prepared 1% w/v carrageenan solution (150  $\mu$ l). The hind-paw volume was measured by vernier caliper before carrageenan injection and then at 1, 2, 4, and 6-h intervals. The % inhibition of edema was calculated as the difference between the groups provided carrageenan alone and carrageenan with treatment in reducing the paw volume. Animals were sacrificed after 6 h and hind paws were collected below the ankle and stored until assayed at  $-80$  °C.

$$\text{Percent edema} = \frac{C - T}{C} \times 100,$$

where “C” is the mean increase in the volume of the paw in control rats and “T” is the mean increase in the volume of the paw in treated rats.

#### Ulcerogenicity study

The ulcerogenic assay of compound **7h** was studied in male Wistar rats of weight 150–180 g according to Ganguly and Bhatnagar [36] with slight modification. The Wistar rats were randomly separated into four sets of five in each. Group I control, group II and III received compound **7h** at 10 and 50 mg/kg, and group IV administered with indomethacin 10-mg/kg daily orally for 7 successive days. The study was carried out on fasting animals. Animals have sacrificed after 4 h later the last dose by cervical dislocation. The stomach was separated and cleaned with cooled saline by making a longitudinal incision along the greater curvature. The gastric mucosa was examined under the magnifying lens for any evidence of ulcer. Besides, histopathological studies were carried out using hematoxylin and eosin [37–39].

#### PGE<sub>2</sub> and LTB<sub>4</sub> screening assay in rat-paw tissues

Hind-paw tissues frozen at  $-80$  °C were brought to RT and degloved the bone to separate the tissues. The tissues were then homogenized in 5-mL ice-cold saline and suspended for 10 min in acetone at RT. Subsequently, the

homogenized tissue was centrifuged for 10 min at 2000 *g* at 4 °C. PGE<sub>2</sub> and LTB<sub>4</sub> were measured using the ELISA technique from supernatants aliquot by PGE<sub>2</sub> and leukotriene B<sub>4</sub> parameter kits according to the manufacturer's instruction [33, 40] (Catalog No. KGE004B & KGE006B, R&D systems, Inc. USA). PGE<sub>2</sub> and LTB<sub>4</sub> production were determined in duplicates and concentrations were obtained from PGE<sub>2</sub> or LTB<sub>4</sub> standard curve [41].

### Total RNA isolation and cDNA synthesis

The total RNA was isolated from the rat-paw tissues stabilized by RNA later (Qiagen, USA) using Trizol Reagent (Invitrogen, USA) according to manufactures guidelines. The quality and quantity of the RNA were analyzed by measuring its absorption at A260/A280 nm by Nanodrop BioSpectrometer (Eppendorf BioSpectrometer®, USA) as well as with agarose gel separation. cDNA synthesis was performed with 2 µg of total RNA from each sample using the Omniscript Reverse Transcription kit (Qiagen, USA) according to manufactures guidelines. Briefly, 20-µl reaction was performed using 2-µg total RNA, 10-µM oligo dT primer (Qiagen), 5-mM dNTP mix, 10× buffer RT, Omniscript reverse transcriptase, RNase inhibitor, and RNase free water and incubated for 60 min at 37 °C.

### Gene expression analysis in Wistar rat

qRT-PCR reactions were carried out to study the expression of three target genes and one internal control (GAPDH). Primers for each gene were designed using NCBI primer BLAST software. All primers were obtained from Eurofins Genomics India Pvt. Ltd. (Bangalore, India). The reverse-transcribed cDNA from rat-paw tissues treated with the test, standard, and control was used as the template for determining the expression of COX-1, COX-2, and 5-LOX, and GAPDH. The amplifications were carried out in 0.2-ml qPCR 8-strips tubes with optical caps (Gunster Biotech Co., Ltd, Taiwan) using the CFX96 Real-Time System (BIORAD, USA). The real-time PCR reactions were carried out in 25-µL reaction systems with TB Green Premix Ex Taq II, 12.5 µL (Takara Bio Inc., Japan), 200-ng forward primer (10 µM), 200-ng reverse primer (10 µM), and 2-µL cDNA template. Each reaction was performed in triplicate. Thermal cycling conditions were; initial denaturation 95 °C for 30 s, subsequently 40 cycles of denaturation at 95 °C for 10 s, annealing at 60 °C for 1 min, and a final extension at 95 °C for 10 s. A PCR product melt curve analysis was done by heating from 65 to 95 °C with increments of 0.5 s. Data analysis was performed with the BIORAD CFX Maestro™ 4.1.2 (Bio-Rad). The quantification of studied enzyme gene expression was performed using the housekeeping gene GAPDH [42]. The  $2^{-\Delta\Delta C_t}$  method was used for gene expression ratio

calculation [42–44]. Relative amounts of all target genes were expressed by normalizing to GAPDH and control gene levels. Primers used are according to the previous report [27].

### MTT assay

#### Cell culture

A549 (Lung Cancer), MCF-7 (Human Breast Adenocarcinoma), DLD1 (Human Colorectal Adenocarcinoma), and L929 (Fibroblast) cells were obtained from NCCS, Pune, India and maintained in DMEM (Sigma Aldrich, USA). The cells were cultured in DMEM supplemented with L-glutamine, 10% FBS, sodium bicarbonate, and 1% antibiotic solution (Streptomycin, 100 µg/ml, Penicillin, 100 U/ml, and Amphotericin B, 2.5 µg/ml) maintained at 37 °C under 5% CO<sub>2</sub> incubator.

#### Cell proliferation assay

The cytotoxicity and anti-proliferative activities of the most active compound **7h** were studied against L929, A549, MCF-7, and DLD1 cells by a modified standard MTT assay. Briefly, 96-well tissue culture plates were seeded with 100-µl cell suspension ( $5 \times 10^4$  cells/well) and incubated under 5% CO<sub>2</sub> incubator at 37 °C. After 24 h, compounds were added by serial dilution (100, 50, 25, 12.5, 6.25 µM) to the cells maintained in fresh 5% DMEM and incubated at 37 °C under 5% CO<sub>2</sub> incubator. Non-treated control cells were also maintained. At the end of the incubation period, 30 µl of reconstituted MTT solution (5 mg/mL in PBS) was added to all the wells and incubated for 4 h under 5% CO<sub>2</sub> at 37 °C. Then, developed formazan crystals were solubilized by adding 100 µl of DMSO. The absorbance was read on a microplate reader (ERBA, Germany) at 540 nm [45].

The percentage of cell viability was calculated using the formula:

$$\frac{\text{Mean OD samples}}{\text{Mean OD of control group}} \times 100.$$

### Determination of antioxidant activity

#### DPPH free radical scavenging assay

The synthesized compounds have been studied for DPPH free radical scavenging efficiency as reported [25, 46]. Briefly, equal volumes of test compounds dissolved in methanol (20 µM) and freshly prepared DPPH (0.1 mM) were mixed thoroughly and kept for 30 min in the dark at RT. The absorbance was determined on a UV–visible spectrophotometer (Shimadzu, Japan) at 517 nm. The standard used was ascorbic acid and experiments were

carried out in triplicate. The percent DPPH radical scavenging was calculated by the formula:

$$\% \text{ inhibition} = \frac{(A_0 - A_s)}{A_0} \times 100, \quad (1)$$

where  $A_0$  = absorbance of the control and  $A_s$  = absorbance of the test or standard sample.

### H<sub>2</sub>O<sub>2</sub> radical scavenging assay

H<sub>2</sub>O<sub>2</sub> scavenging assay was performed for all the test compounds at 20- $\mu$ M concentration according to earlier-reported method with minor modification [46]. In brief, 1-ml H<sub>2</sub>O<sub>2</sub> solution (40 mM) in PBS (pH 7.4) and 1-ml test compounds in DMSO were mixed well and developed at RT for 10 min. The concentration of H<sub>2</sub>O<sub>2</sub> was spectrophotometrically determined at 230 nm against PBS solution without H<sub>2</sub>O<sub>2</sub> as blank. Triplicate experiments were conducted and results are displayed as mean  $\pm$  SD. The percentage scavenging activity was determined by Eq. (1).

### Iron-chelating assay

All compounds synthesized were assessed for iron (II) chelating assay according to Chew et al. [47]. Briefly, 1-ml 0.1-mM ferrous sulfate, 1-ml test compound (20  $\mu$ M), and 1-ml 0.25-mM ferrozine were mixed well and allowed to stand for 10 min. Absorbance was observed spectrophotometrically at 562 nm. The iron (II) chelating activity was calculated by Eq. (1), where control consists of 1 ml each of 75% methanol, 0.1-mM ferrous sulfate, and 0.25-mM ferrozine.

### Nitric oxide (NO) scavenging assay

The nitric oxide scavenging activity of all the newly synthesized molecules was measured by previous reports [48]. Briefly, 0.8 ml of test compounds (20  $\mu$ M) in methanol was mixed with 0.2 ml of 5-mM sodium nitroprusside in PBS (pH 7.4) and incubated at RT for 180 min under a light source. After incubation, 0.6 ml of the above mixture was mixed with 0.6 ml of Griess reagent and incubated in dark for 10 min. The absorbance was spectrophotometrically observed at 546 nm. The nitrite radical generated with or without test compounds was estimated by plotting a standard curve with known concentrations of sodium nitrite solution. Experiments were performed in triplicate and the percentage of nitrite scavenging was calculated.

### Molecular docking studies

A molecular docking study was performed by using AutoDockTools-1.5.6. The crystal structures used for COX-

2 and 5-LOX enzymes were PDB ID: 5IKT and PDB ID: 3O8Y acquired from the protein data bank, respectively. Briefly, the preparation of ligands, **7h**, and reference drugs and energy minimization was carried out using the Argus Lab 4.0.1 and Swiss-Pdb viewer 4.1.0, respectively. The ligands were docked to predefined active sites [25], where polar hydrogens and partial charges were added to protein and ligands. Grid maps of  $60 \times 60 \times 60 \text{ \AA}^3$  points were centered on the protein active sites. Ligand conformational search was performed by the Lamarckian Genetic Algorithm. The genetic algorithm (GA) population size was fixed to 150, the number of GA evaluation as 2500,000, and GA docking runs were set to 100. To understand the mode of interaction each ligand was docked separately with the enzymes. After docking, the binding energies of the ligands at different enzyme active sites were analyzed. The hydrophilic and hydrophobic interactions as well as van der Waal's interaction were explored by measuring the distance between the protein and ligand [49].

### Conclusion

In the current study, we successfully designed and synthesized a series of new thiazoles and thiazolidenes from thiourea by solvent-free conditions. All the synthesized molecules were evaluated for in vitro COX-2 and 5-LOX inhibition. Among them, (2-(diphenylamino)-4-(4-nitrophenyl)thiazol-5-yl)(naphthalen-1-yl)methanone, **7h** with two bulky groups such as diphenylamino group and naphthoyl group on thiazole ring showed the best dual inhibitory activity with COX-2  $IC_{50} = 0.07 \pm 0.02 \mu\text{M}$  and 5-LOX  $IC_{50} = 0.29 \pm 0.09 \mu\text{M}$ . Besides, compound **7h** has revealed a superior COX-1/COX-2 selectivity index of 115.14 compared to the reference drug etoricoxib, 91.28. The PGE<sub>2</sub> and LTB<sub>4</sub> inhibition studies on LPS-induced RAW 264.7 cells exhibited significant activity, specifically compound **7h**. Meanwhile, in vivo acute toxicity studies on male Wistar rats showed no indication of toxicity. In vivo anti-inflammatory studies showed that **7h** could reduce the inflammation induced by carrageenan in male Wistar rats effectively (63%) compared to indomethacin at the same doses. Furthermore, the antiulcer studies and histopathological analysis showed superior gastric protection of **7h** than indomethacin. The qRT-PCR studies, PGE<sub>2</sub>/LTB<sub>4</sub> inhibition assays on paw tissues of Wistar rats obtained after anti-inflammatory studies depicted parallel results to in vitro investigations. There was a significant decrease in the expression levels of COX-2 and 5-LOX genes. Besides, the anticancer studies of **7h** on various cell lines displayed moderate inhibition of proliferation, which gains significance with its potent anti-inflammatory activity. On molecular docking studies, the predicted lead **7h** illustrated

excellent interaction with COX-2 and 5-LOX active sites. Moreover, the inclusion of naphthoyl moiety instead of thiophene carbonyl group of our previous study exhibited an overall improvement in the anti-inflammatory activity along with anticancer potency. These results indicate that compound **7h** could pave a promising way for new, safer anti-inflammatory agent development.

### Statistical analysis

The experimental results of three parallel experiments were presented as mean  $\pm$  SD or otherwise mentioned in the procedure. Animal experiment data were given as mean standard error ( $\pm$ SEM). Statistical evaluation was carried out by one-way analysis of variance. Statistical significance is expressed as  $*p < 0.05$ ,  $**p < 0.01$ , and  $***p < 0.001$ .

**Acknowledgements** The authors greatly acknowledge VIT, Vellore for providing “VIT Seed Grant” for research. Jaismy Jacob P recognizes CSIR, Govt. of India, for the financial support through Senior Research Fellowship for research.

### Compliance with ethical standards

**Conflict of interest** The authors declare that they have no conflict of interest.

**Publisher's note** Springer Nature remains neutral with regard to jurisdictional claims in published maps and institutional affiliations.

### References

- Haeggström JZ, Rinaldo-Matthis A, Wheelock CE, Wetterholm A. Advances in eicosanoid research, novel therapeutic implications. *Biochem Biophys Res Commun.* 2010;396:135–139. <https://doi.org/10.1016/j.bbrc.2010.03.140>.
- Coussens LM, Werb Z. Inflammation and cancer. *Nature.* 2002;420:860–867.
- Mantovani A, Allavena P, Sica A, Balkwill F. Cancer-related inflammation. *Nature.* 2008;54:436. <https://doi.org/10.1038/nature07205>.
- Manju SL, Ethiraj KR, Elias G. Safer anti-inflammatory therapy through dual COX-2/5-LOX inhibitors: a structure-based approach. *Eur J Pharm Sci.* 2018;121:356–381. <https://doi.org/10.1016/j.ejps.2018.06.003>.
- Singh P, Kaur J, Singh G, Bhatti R. Triblock conjugates: identification of a highly potent antiinflammatory agent. *J Med Chem.* 2015;58:5989–6001. <https://doi.org/10.1021/acs.jmedchem.5b00952>.
- Ding X, Zhu C, Qiang H, Zhou X, Zhou G. Enhancing antitumor effects in pancreatic cancer cells by combined use of COX-2 and 5-LOX inhibitors. *Biomed Pharmacother.* 2011;65:486–490. <https://doi.org/10.1016/j.biopha.2011.06.009>.
- Chang J, Tang N, Fang Q, Zhu K, Liu L, Xiong X, et al. Inhibition of COX-2 and 5-LOX regulates the progression of colorectal cancer by promoting PTEN and suppressing PI3K/AKT pathway. *Biochem Biophys Res Commun.* 2019;517:1–7. <https://doi.org/10.1016/j.bbrc.2018.01.061>.
- Harris RE, Beebe-Donk J, Alshafie GA. Cancer chemoprevention by cyclooxygenase 2 (COX-2) blockade. In: *Inflammation in the pathogenesis of chronic diseases, Subcellular Biochemistry.* vol 42. Springer, Dordrecht. 2007. pp. 193–212. [https://doi.org/10.1007/1-4020-5688-5\\_9](https://doi.org/10.1007/1-4020-5688-5_9).
- Omar YM, Abdel-Moty SG, Abdu-Allah HH. Further insight into the dual COX-2 and 15-LOX anti-inflammatory activity of 1, 3, 4-thiadiazole-thiazolidinone hybrids: the contribution of the substituents at 5th positions is size dependent. *Bioorg Chem.* 2020;97:103657. <https://doi.org/10.1016/j.bioorg.2020.103657>.
- de Souza MVN. Synthesis and biological activity of natural thiazoles: an important class of heterocyclic compounds. *J Sulphur Chem.* 2005;26:429–449. <https://doi.org/10.1080/17415990500322792>.
- Kouatly O, Geronikaki A, Kamoutsis C, Hadjipavlou-Litina D, Eleftheriou P. Adamantane derivatives of thiazolyl-N-substituted amide, as possible non-steroidal anti-inflammatory agents. *Eur J Med Chem.* 2009;44:1198–1204. <https://doi.org/10.1016/j.ejmech.2008.05.029>.
- T Chhabria M, Patel S, Modi P, S Brahmshatriya P. Thiazole: a review on chemistry, synthesis and therapeutic importance of its derivatives. *Curr Top Med Chem.* 2016;16:2841–2862.
- Hsu A, Granneman GR, Bertz RJ. Ritonavir. *Clin Pharmacokinet.* 1998;35:275–291. <https://doi.org/10.2165/00003088-199835040-00002>.
- Gündüz MG, Tahir MN, Armarković S, Koçak CÖ, Armarković SJ. Design, synthesis and computational analysis of novel acridine-(sulfadiazine/sulfathiazole) hybrids as antibacterial agents. *J Mol Struct.* 2019;1186:39–49. <https://doi.org/10.1016/j.molstruc.2019.03.010>.
- Borelli C, Schaller M, Niewerth M, Nocker K, Baasner B, Berg D, et al. Modes of action of the new arylguanidine abafungin beyond interference with ergosterol biosynthesis and in vitro activity against medically important fungi. *Chemotherapy.* 2008;54:245–259. <https://doi.org/10.1159/000142334>.
- Noble S, Balfour J. Meloxicam. *Drugs.* 1996;51:424–430.
- Hubble JP, Koller WC, Cutler NR, Sramek JJ, Friedman J, Goetz C, et al. Pramipexole in patients with early Parkinson's disease. *Clin Neuropharmacol.* 1995;18:338–347. <https://doi.org/10.1097/00002826-199508000-00006>.
- O'Dwyer PJ, Shoemaker DD, Jayaram HN, Johns DG, Cooney DA, Marsoni S, et al. Tiazofurin: a new antitumor agent. *Invest New Drugs.* 1984;2:79–84. <https://doi.org/10.1007/BF00173791>.
- Stubbe J, Kozarich JW. Mechanisms of bleomycin-induced DNA degradation. *Chem Rev.* 1987;87:1107–1136. <https://doi.org/10.1021/cr00081a011>.
- Liaras K, Fesatidou M, Geronikaki A. Thiazoles and thiazolidinones as COX/LOX inhibitors. *Molecules.* 2018;23:685. <https://doi.org/10.3390/molecules23030685>.
- Woods KW, McCroskey RW, Michaelides MR, Wada CK, Hulkower KI, Bell RL. Thiazole analogues of the NSAID indomethacin as selective COX-2 inhibitors. *Bioorg Med Chem Lett.* 2001;11:1325–1328. [https://doi.org/10.1016/S0960-894X\(01\)00212-8](https://doi.org/10.1016/S0960-894X(01)00212-8).
- Abdelall EK, Kamel GM. Synthesis of new thiazolo-celecoxib analogues as dual cyclooxygenase-2/15-lipoxygenase inhibitors: determination of regio-specific different pyrazole cyclization by 2D NMR. *Eur J Med Chem.* 2016;118:250–258. <https://doi.org/10.1016/j.ejmech.2016.04.049>.
- Afifi OS, Shaaban OG, El Razik HAA, El SE-DAS, Ashour FA, El-Tombary AA, Abu-Serie MM. Synthesis and biological evaluation of purine-pyrazole hybrids incorporating thiazole, thiazolidinone or rhodanine moiety as 15-LOX inhibitors endowed with anticancer and antioxidant potential. *Bioorg Chem.* 2019;87:821–837. <https://doi.org/10.1016/j.bioorg.2019.03.076>.
- Sinha S, Sravanthi T, Yuvaraj S, Manju S, Doble M. 2-Amino-4-aryl thiazole: a promising scaffold identified as a potent 5-LOX inhibitor. *RSC Adv.* 2016;6:19271–19279. <https://doi.org/10.1039/C5RA28187C>.
- Sinha S, Doble M, Manju S. Design, synthesis and identification of novel substituted 2-amino thiazole analogues as potential anti-

- inflammatory agents targeting 5-lipoxygenase. *Eur J Med Chem.* 2018;158:34–50. <https://doi.org/10.1016/j.ejmech.2018.08.098>.
26. Sinha S, Manju S, Doble M. Chalcone-thiazole hybrids: rational design, synthesis and lead identification against 5-lipoxygenase. *ACS Med Chem Lett.* 2019;10:1415–1422. <https://doi.org/10.1021/acsmchemlett.9b00193>.
  27. Jacob PJ, Manju SL. Identification and development of thiazole leads as COX-2/5-LOX inhibitors through in-vitro and in-vivo biological evaluation for anti-inflammatory activity. *Bioorg Chem.* 2020;100:103882. <https://doi.org/10.1016/j.bioorg.2020.103882>.
  28. Zhang P, Ye D, Chu Y. An efficient one-pot procedure for the synthesis of 1, 5-benzothiazepinones catalyzed by tetrabutylammonium fluoride (TBAF). *Tetrahedron Lett.* 2016;57:3743–3745. <https://doi.org/10.1016/j.tetlet.2016.07.012>.
  29. Bramley SE, Dupplin V, Goberdhan DG, Meakins GD. The Hantzsch thiazole synthesis under acidic conditions: change of regioselectivity. *J Chem Soc [Perkin Trans 1].* 1987;1:639–643. <https://doi.org/10.1039/P19870000639>.
  30. Brindley JC, Caldwell JM, Meakins GD, Plackett SJ, Price SJ. N'-substituted N-acyl-and N-imidoyl-thioureas: preparation and conversion of N', N'-disubstituted compounds into 2-(N, N-disubstituted amino) thiazol-5-yl ketones. *J Chem Soc [Perkin Trans 1].* 1987;1:1153–1158. <https://doi.org/10.1039/P19870001153>.
  31. Pan Y, Li H, Zheng S, Zhang B, Deng Z-y. Implication of the significance of dietary compatibility: based on the antioxidant and anti-inflammatory interactions with different ratios of hydrophilic and lipophilic antioxidants among four daily agricultural crops. *J Agr Food Chem.* 2018;66:7461–7474. <https://doi.org/10.1021/acs.jafc.8b01690>.
  32. Singh P, Prasher P, Dhillon P, Bhatti R. Indole based peptidomimetics as anti-inflammatory and anti-hyperalgesic agents: dual inhibition of 5-LOX and COX-2 enzymes. *Eur J Med Chem.* 2015;97:104–123. <https://doi.org/10.1016/j.ejmech.2015.04.044>.
  33. Xu G-L, Liu F, Ao G-Z, He S-Y, Ju M, Zhao Y, Xue T. Anti-inflammatory effects and gastrointestinal safety of NNU-hdpa, a novel dual COX/5-LOX inhibitor. *Eur J Pharmacol.* 2009;611:100–106. <https://doi.org/10.1016/j.ejphar.2009.03.062>.
  34. Abdelall EK. Synthesis and biological evaluations of novel isoxazoles and furoxan derivative as anti-inflammatory agents. *Bioorg Chem.* 2020;94:103441. <https://doi.org/10.1016/j.bioorg.2019.103441>.
  35. Abdelrahman MH, Youssif BG, Abdelazeem AH, Ibrahim HM, Abd El Ghany AM, Treambu L, Bukhari SNA. Synthesis, Biological evaluation, docking study and ulcerogenicity profiling of some novel quinoline-2-carboxamides as dual COXs/LOX inhibitors endowed with anti-inflammatory activity. *Eur J Med Chem.* 2017;127:972–985. <https://doi.org/10.1016/j.ejmech.2016.11.006>.
  36. Ganguly A, Bhatnagar O. Effect of bilateral adrenalectomy on production of restraint ulcers in the stomach of albino rats. *Can J Physiol Pharm.* 1973;51:748–750. <https://doi.org/10.1139/y73-113>.
  37. Ganguly A. A method for quantitative assessment of experimentally produced ulcers in the stomach of albino rats. *Experientia.* 1969;25:1224.
  38. Sabt A, Eldehna WM, Al-Warhi T, Alotaibi OJ, Elaasser MM, Suliman H, et al. Discovery of 3, 6-disubstituted pyridazines as a novel class of anticancer agents targeting cyclin-dependent kinase 2: synthesis, biological evaluation and in silico insights. *J Enzyme Inhib Med Chem.* 2020;35:1616–1630. <https://doi.org/10.1080/14756366.2020.1806259>.
  39. Shrivastava SK, Srivastava P, Bandresh R, Tripathi PN, Tripathi A. Design, synthesis, and biological evaluation of some novel indolizine derivatives as dual cyclooxygenase and lipoxygenase inhibitor for anti-inflammatory activity. *Bioorg Med Chem.* 2017;25:4424–4432. <https://doi.org/10.1016/j.bmc.2017.06.027>.
  40. Lee ES, Park BC, Paek SH, Lee YS, Basnet A, Jin DQ, et al. Potent analgesic and anti-inflammatory activities of 1-furan-2-yl-3-pyridin-2-yl-propenone with gastric ulcer sparing effect. *Biol Pharm Bull.* 2006;29:361–364. <https://doi.org/10.1248/bpb.29.361>.
  41. Larré S, Tran N, Fan C, Hamadeh H, Champigneulle J, Azzouzi R, et al. PGE2 and LTB4 tissue levels in benign and cancerous prostates. *Prostaglandins Other Lipid Mediat.* 2008;87:14–19. <https://doi.org/10.1016/j.prostaglandins.2008.05.001>.
  42. Livak KJ, Schmittgen TD. Analysis of relative gene expression data using real-time quantitative PCR and the 2<sup>-</sup>ΔΔCT method. *Methods.* 2001;25:402–408. <https://doi.org/10.1006/meth.2001.1262>.
  43. Dhanamjayulu P, Boga RB, Mehta A. Inhibition of aflatoxin B1 biosynthesis and down regulation of aflR and aflB genes in presence of benzimidazole derivatives without impairing the growth of *Aspergillus flavus*. *Toxicon.* 2019;170:60–67. <https://doi.org/10.1016/j.toxicon.2019.09.018>.
  44. Karthikeyan K, Sudhakaran R. Experimental horizontal transmission of *Enterocytozoon hepatopenaei* in post-larvae of white-leg shrimp, *Litopenaeus vannamei*. *J Fish Dis.* 2019;42:397–404. <https://doi.org/10.1111/jfd.12945>.
  45. Sasidharan R, Sreedharannair Leelabaiamma M, Mohanan R, Jose SP, Mathew B, Sukumaran S. Anti-inflammatory effect of synthesized indole-based chalcone (2E)-3-(4-bromophenyl)-1-(1H-indol-3-yl) prop-2-en-1-one: an in vitro and in vivo studies. *Immunopharmacol Immunotoxicol.* 2019;2019:1–9. <https://doi.org/10.1080/08923973.2019.1672177>.
  46. Adjimani JP, Asare P. Antioxidant and free radical scavenging activity of iron chelators. *Toxicol Rep.* 2015;2:721–728. <https://doi.org/10.1016/j.toxrep.2015.04.005>.
  47. Chew Y-L, Goh J-K, Lim Y-Y. Assessment of in vitro antioxidant capacity and polyphenolic composition of selected medicinal herbs from Leguminosae family in Peninsular Malaysia. *Food Chem.* 2009;116:13–18. <https://doi.org/10.1016/j.foodchem.2009.01.091>.
  48. Chai T-T, Wong F-C. Whole-plant profiling of total phenolic and flavonoid contents, antioxidant capacity and nitric oxide scavenging capacity of *Turnera subulata*. *J Med Plant Res.* 2012;6:1730–1735. <https://doi.org/10.5897/JMPR11.1541>.
  49. Jan MS, Ahmad S, Hussain F, Ahmad A, Mahmood F, Rashid U, et al. Design, synthesis, in-vitro, in-vivo and in-silico studies of pyrrolidine-2, 5-dione derivatives as multitarget anti-inflammatory agents. *Eur J Med Chem.* 2020;186:111863. <https://doi.org/10.1016/j.ejmech.2019.111863>.
  50. Wu SY, Zhao XY, Li HP, Yang Y, Roesky HW. Synthesis and Characterization of N, N-Di-substituted Acylthiourea Copper (II) Complexes. *Z Anorg Allg Chem.* 2015;641(5):883–889. <https://doi.org/10.1002/zaac.201400605>.
  51. Bai L, Li S, Wang JX, Chen M. Synthesis of benzoyl-N-phenylthioureas under microwave irradiation and phase transfer catalysis conditions. *Synth. Commun.* 2002;32(1):127–132. <https://doi.org/10.1081/SCC-120001519>.
  52. Dzurilla M, Kutschy P, Imrich J, Brtoš S. Hagershoff Reaction of N-1-or N-2-Naphthoyl-N'-monosubstituted and N', N'-Disubstituted Thiourea Derivatives. *Collect. Czech. Chem. Commun.* 1994;59(12):2663–2676. <https://doi.org/10.1135/cccc19942663>.
  53. Hemdan MM, Fahmy AF, El-Sayed AA. Synthesis and antimicrobial study of 1, 2, 4-triazole, quinazoline and benzothiazole derivatives from 1-naphthoylthiocyanate. *J. Chem. Res.* 2010;34(4):219–221. <https://doi.org/10.3184/030823410X12707543946812>.